SURFACE AND SMALL-SCALE PROCESSES OF BIOGEOCHEMICAL CYCLING OF ORGANIC MATTER IN TIDAL MARSH SEDIMENTS

Gwendolyn A. Shaughnessy

A Thesis Submitted to the
University of North Carolina Wilmington in Partial Fulfillment
Of the Requirements for the Degree of
Master of Science

Department of Chemistry and Biochemistry

University of North Carolina Wilmington

2007

Approved by

Advisory Committee

Dr. Stephen Skrabal	Dr. G. Brooks Avery
Co-Chair	Co-Chair

Dr. Courtney Hackney

Accepted by

_____
Dean, Graduate School

TABLE OF CONTENTS

ABSTRACT

Despite their exceptionally high productivity, freshwater and oligohaline tidal marshes are rarely studied in terms of their biogeochemistry because of their highly variable and diverse conditions. Such environments are particularly interesting because they experience salinity variations that can dramatically alter biogeochemical processes. Sediment cores were collected on a monthly basis over the course of one year from three substations (intertidal mud flat, marsh, and marsh/upland edge) of an oligohaline tidal marsh in the Cape Fear River Estuary, North Carolina. Depth profiles of redox-active remineralization products (O_2, Fe^{2+}, Mn^{2+}, and HS^-) were generated with microelectrode-based voltammetry, allowing for high-resolution (millimeter scale) assessment of small-scale microbial processes often overlooked in biogeochemical studies. Oxygen (and attendant aerobic respiration), when present, was limited to less than 7 mm below the sediment-water interface at all three substations. Low quantities of labile organic matter limited remineralization processes to Mn reduction in the upper 10 cm of the intertidal mud flat sediments; Fe reduction and sulfate reduction play apparently minor roles. While Mn reduction has previously been shown to dominate organic matter remineralization in some coastal marine sediments, this study demonstrates that this process is also important in intertidal mud flat sediments. Seasonal trends emerged in the biogeochemistry of the marsh substation due to sediment-root interactions, in which sulfate reduction dominated in spring and summer, Mn reduction in fall, and methane production in winter. Marsh/upland edge sediments were highly influenced by subsurface hydrology and plant physiology, resulting in a biogeochemical mosaic of overlapping microenvironments dominated by different remineralization pathways (Mn reduction, Fe reduction, sulfate reduction, methanogenesis). Biogeochemistry at this substation reflects changes in environmental conditions on short time scales due to subsurface hydrology,

tidal inundation, plant physiology, rainfall, and labile organic matter content. These sites and their varied biogeochemistry are likely to represent transitional environments expected to result from sea level rise. The great complexity of these environments, as demonstrated in this study, creates challenges for predicting the role that transitional wetlands will play in carbon storage and the release of greenhouse gases.

ACKNOWLEDGEMENTS

My special thanks go to my family and friends for their support and encouragement through this chapter in my life. It has been a long and challenging road, and I hope they know what they mean to me and how much strength they lend me. I could not have succeeded in this endeavor without their influence.

I would also like to thank my committee for their tireless guidance and assistance with this project. I would not have been able to wade through all the electrochemistry without Dr. Stephen Skrabal's contribution and infinite wisdom. I would like to extend special thanks to Dr. Courtney Hackney's lab team for taking me out to the study site to collect cores.

Finally, I would like to thank the Center for Marine Science, MACRL, and the Graduate School for financial support of this project.

DEDICATION

I would like to dedicate this thesis in loving memory to my father, Dale J. Shaughnessy. His love, laughter, and guidance are missed more than he will ever know.

LIST OF TABLES

LIST OF FIGURES

INTRODUCTION

Estuarine wetlands are regarded as some of the most productive ecosystems in the world. Although salt marshes have been well studied in terms of aboveground and belowground biomass and production (e.g., Schubauer and Hopkinson, 1984; Valiela et al., 1976; de la Cruz and Hackney, 1977), less information is available on productivity in freshwater and oligohaline tidal marsh systems. Production in these ecosystems is difficult to study because they typically have high plant species diversity, seasonally variable species composition, and extensive yet patchy belowground biomass. Although freshwater tidal marshes appear highly diverse in terms of net carbon production rates (Whigham et al., 1978; Doumlete, 1981; Chanton et al., 1992), research suggests that they are as productive as salt marshes, when both aboveground and belowground production are considered (Flemer et al.,1978; Neubauer, 2000).

Tidal marshes may function as carbon sinks during sea-level rise by the accretion of organic matter and sediment (Rabenhorst, 1995). Sediments in tidal marshes are characteristically waterlogged, resulting in anoxic and reducing conditions (Mitsch and Gosselink, 1993). Organic matter decomposition rates in these anoxic sediments are typically slow, favoring the accumulation of organic matter. Hussein et al. (2004) speculated that coastal marsh ecosystems may accumulate and efficiently sequester atmospheric carbon and thereby impact global climate change. How organic matter is cycled in these systems is essential to understanding their role in the global carbon cycle (e.g. Brasse et al., 2002; Wang and Cai, 2004).

The fate of organic carbon in wetlands may have profound implications for the global carbon cycle. Integrating wetland carbon dynamics into global predictive models is difficult because there are many types of wetlands, and their responses to climate change remain

uncertain (MRCSP, 2005; Reed and Cahoon, 1999). Also, net carbon sequestering and/or release in wetlands involve complex processes that depend on the interaction of several environmental parameters and processes.

Sedimentary organic matter decomposition in tidal marshes, as in all sediments, is regulated by a series of microbially-mediated processes (Froelich et al., 1979; Berner, 1980). In a closed system the sequence of reactions can be predicted based on thermodynamic properties (Table 1). Sediments with undisturbed conditions at the sediment-water interface demonstrate a corresponding depth distribution to this sequence of reactions (Figure 1.). If oxygen (O_2) is present, aerobic decomposition is the first step in breaking down organic matter. As dissolved O_2 becomes sufficiently depleted, further organic decomposition continues via nitrate reduction. As nitrate is exhausted, iron (Fe) and manganese (Mn) oxides serve as the major oxidants. When metal oxides are no longer available, organic matter degradation proceeds through sulfate reduction (SR) and ends with methanogenesis as the final reaction in the series.

The vertical biogeochemical zonation described above, however, relies on the existence of steady-state conditions which may not exist in estuarine environments (Sundby, 2006). Physical environmental conditions of these systems, including temperature, salinity, organic matter deposition, and chemical compositions, can vary by season. Furthermore, estuaries are subject to random and periodic large-scale disturbances such as storms and spring tides which can influence bottom current velocities and the subsequent resuspension and scouring of surface sediments. The biogeochemistry of estuarine surface sediments is also impacted by small-scale disturbances including bioturbation and plant physiology (e.g. Howes, 1986; Koretsky et al., 2002; Roden and Wetzel, 1996; Kristensen, 2000). These factors combine to create a

biogeochemical mosaic of microenvironments, rather than a vertically stratified distribution (Aller, 1982).

Most early research on the pathways of organic matter remineralization in estuarine sediments has focused on only the anoxic processes. It was generalized that salt marsh sediments are dominated by SR (e.g., Jorgensen, 1982; Howarth, 1984), whereas methanogenesis dominates in freshwater tidal marshes (e.g., Kelley et al., 1990; Lovely and Klug, 1986; Capone and Kiene, 1988). Oxic and suboxic processes have been commonly discounted as major contributors to decomposition in both types of systems and remain poorly characterized.

Oxygen is utilized rapidly in organic-rich surface sediments, usually restricting aerobic respiration to the top few millimeters below the sediment-water interface (King, 1988). Dissimilatory nitrate reduction does not support a significant fraction of carbon oxidation due to typically low concentrations of nitrate in overlying water and porewater (Sorensen et al., 1979). This process is typically limited to a narrow zone below the depth of O_2 penetration, contributing very little to sediment diagenesis (Canfield et al., 1993). Although a few studies have reported instances of high allochthonous nitrate inputs resulting in nitrate reduction being a key step in the bacterial transformation of organic matter (Jorgensen and Sorensen, 1985; Capone and Bautista, 1985), nitrate processes and cycles are primarily studied in terms of nutrient dynamics for marsh vegetation (Canfield et al., 1993).

Table 1. Free energy changes (ΔG°) for bacterial oxidation reactions of organic matter, adapted from Froelich et al. (1979).

Reaction	ΔG° (kJ/mol) glucose
Aerobic Respiration $(CH_2O)_{106}(NH_3)_{16}(H_3PO_4) + 138O_2 \rightarrow 106CO_2 + 16HNO_3 + H_3PO_4 + 122H_2O$	-3190
Manganese Reduction $(CH_2O)_{106}(NH_3)_{16}(H_3PO_4) + 236MnO_2 + 472H^+ \rightarrow 236Mn^{2+} + 106CO_2 + 8N_2 + H_3PO_4 + 366H_2O$	-3090
Nitrate Reduction $(CH_2O)_{106}(NH_3)_{16}(H_3PO_4) + 94.4HNO_3 \rightarrow 106CO_2 + 55.2N_2 + H_3PO_4 + 177.2\ H_2O$	-3030
Iron Reduction $(CH_2O)_{106}(NH_3)_{16}(H_3PO_4) + 212Fe_2O_3 + 848H^+ \rightarrow 424Fe^{2+} + 106CO_2 + 16NH_3 + H_3PO_4 + 530H_2O$	-1410
$(CH_2O)_{106}(NH_3)_{16}(H_3PO_4) + 424FeOOH + 848H^+ \rightarrow 424Fe^{2+} + 106CO_2 + 16NH_3 + H_3PO_4 + 742H_2O$	-1330
Sulfate Reduction $(CH_2O)_{106}(NH_3)_{16}(H_3PO_4) + 53SO_4^{2-} \rightarrow 106CO_2 + 16NH_3 + 53S^- + H_3PO_4 + 106H_2O$	-380
Methanogenesis $(CH_2O)_{106}(NH_3)_{16}(H_3PO_4) \rightarrow 53CO_2 + 53CH_4 + 16NH_3 + H_3PO_4$	-350

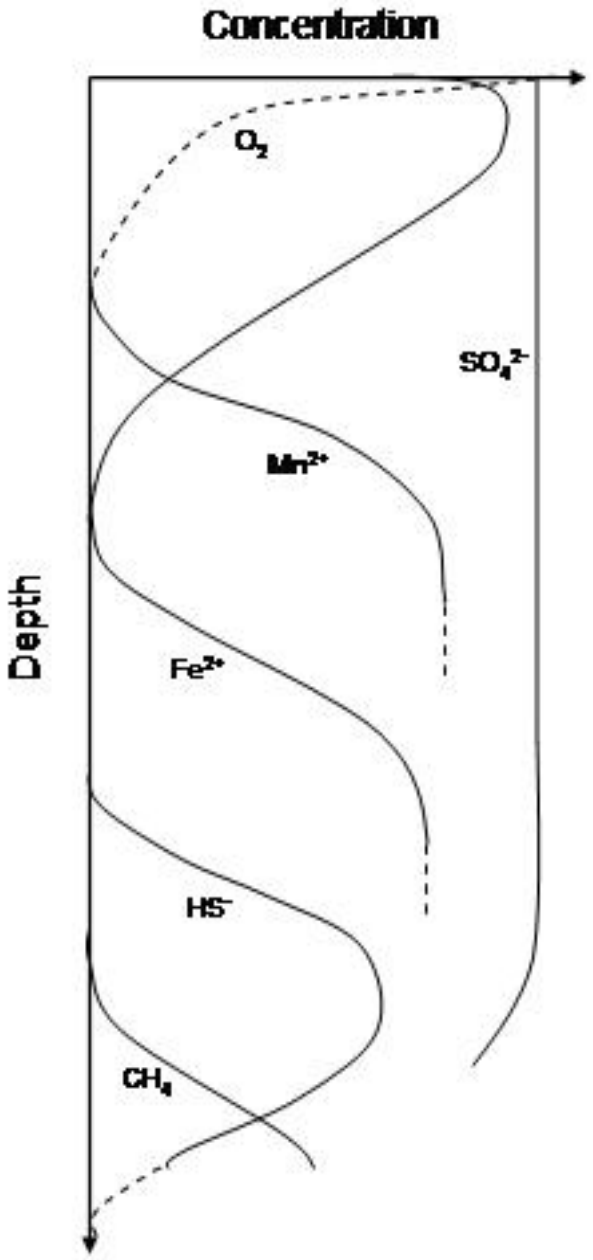

Figure 1. Hypothetical pore water profiles of oxidants predicted by the successive utilization of inorganic compounds as terminal electron acceptors in sedimentary organic matter decomposition (modified from Froelich et al., 1979).

Recently, microbial manganese (Mn) and iron (Fe) reduction have been demonstrated as dominant pathways in organic matter oxidation in certain marginal marine environments (Hines et al., 1991; Canfield et al., 1993; Aller, 1990; Aller, 1994; Roden & Wetzel, 1996; Thamdrup et al., 1994; Lovely and Phillips, 1986). These studies have shown that in Mn-rich sediments, Mn reduction may be the dominant respiration pathway. Further estimates of bacterial Fe reduction revealed that Fe reduction can be of equal importance to SR in some coastal sediments (Canfield et al., 1993). Due to the particulate nature of Mn and Fe oxides, it appears that bulk transport mechanisms (such as bioturbation) are important regulators of dissimilatory Mn and Fe reduction.

Distinguishing bacterial Mn and Fe reduction from competing abiotic reactions with reduced inorganic compounds has made the quantification of these respiration pathways difficult (Lovely, 1991; Burdige, 1993). A wide range of organic and inorganic compounds are able to chemically reduce Mn and Fe oxides (or oxyhydroxides). The most studied interaction, however, has been the link between Fe and sulfur species cycling. The product of SR is hydrogen sulfide (H_2S), a substance that is toxic to most organisms. The reaction of H_2S with oxidized Fe exerts important controls on the distribution of H_2S in porewaters. Reduction of oxidized Fe in the presence of H_2S promotes the formation of FeS and FeS_2, removing both the toxic H_2S and the availability of Fe particles for bacterial reduction (Jacobson, 1994). In contrast, a few studies have shown that both H_2S and Fe^{2+} reduce Mn oxides rapidly (Lovely and Phillips, 1988). The majority of these studies have been conducted in salt marsh or marine environments, and the importance of such interactions in freshwater and oligohaline tidal marshes are unclear.

Since physical, biological, and chemical processes are intertwined in estuarine environments, high resolution analytical techniques are needed to investigate the roles of various

reactions in the cycling of carbon. Traditional sampling methods, including interstitial water samplers or "peepers" and sediment core processing techniques, have provided a great deal of information on the biogeochemical cycling of certain elements in wetland sediments (Hesslein, 1976). However, these methods are typically time-consuming, disruptive to sediment integrity, and have poor measurement resolution (de Lange et al., 1992; Howes et al., 1985). One of the most significant drawbacks to these methods is the inability to accurately examine the sediment-water interface, which contains organic material that is fresh and therefore the most bioavailable. The recent development of solid Au/Hg voltammetric microelectrodes has addressed these sampling limitations and requirements (Brendel, 1995; Brendel and Luther, 1995). The advantage of the Au amalgam microelectrode is that it allows the investigation of all the primary redox-sensitive analytes, including O_2, Mn^{2+}, Fe^{2+}, and HS^- simultaneously, in real time, and with millimeter spatial resolution.

Au/Hg voltammetric microelectrodes have been successfully used to examine biogeochemical processes in a variety of environmental settings. Measurements in salt marsh and harbor sediment cores confirmed the validity and accuracy of the microelectrode system, and provided the first detailed information on O_2, Mn^{2+}, Fe^{2+}, and HS^- at millimeter depth resolution (Brendel and Luther. 1995; Luther et al.. 1998). Luther et al. (1998) used the microelectrode to determine the three-dimensional distribution of redox species within the sediment mesocosm of an actively irrigated worm burrow. Results indicated how drastically benthic organisms alter small-scale sediment porewater composition by allowing O_2 to diffuse into the sediments through the irrigation of their burrows. Chapman and Van Den Berg (2005) modified the microelectrode system to fit a microbenthic chamber in order to study small-scale benthic fluxes,

allowing fluxes to be determined in a few hours rather than days, and without the need for sample extraction.

Sundby et al. (2003) investigated the root zone of salt marsh sediments by utilizing the microelectrode technique, revealing a strong correlation between the annual cycles of root growth and decay and porewater redox composition. Additionally, small-scale spatial and temporal variability in seagrass beds due to seagrass and sediment interactions have been examined by Herbert et al. (2007). Although solid-state microelectrodes have been used in a variety of environments, they have not been used yet to characterize highly variable freshwater and oligohaline tidal marsh sediments.

The goal of this study was to apply microelectrode-based voltammetry to obtain depth profiles of redox-active species (O_2, Fe^{2+}, Mn^{2+}, and HS^-) whose concentrations are significantly affected by organic matter remineralization processes. Seasonal and spatial variability of these processes were examined in a series of study sites in the upper Cape Fear River Estuary characterized by low, variable salinity, and topography ranging from subtidal to upland. These sites are of particular interest because they experience periodic intrusions of salinity which are expected to become more common as sea level rises. Such shifts may significantly alter the modes of organic matter remineralization, and subsequently, significant changes in sediment geochemistry and marsh ecology (Hussein et al., 2004).

METHODS

Study site

The study site was located on Eagle Island (34°15'31" N, 77°58'43" W) in the Cape Fear River in North Carolina. This site coincides with station P6 of the Wilmington Harbor Monitoring Program (WHMP) (Figure 2; Hackney et al., 2006). Extensive geochemical data is available for this site since it is monitored monthly as part of a US Army Corps of Engineers project. The site represents a transition between saline and freshwater dominated stations that display variable salinity and geochemical conditions. Due to this varied salinity regime, the dominant plant species often shift and respond quickly to adapt to the stressor. The dominant species along the river edge is *Spartina alterniflora*, and transitioning into less salt tolerant species toward the upland including *Scirpus* sp., *Typha* sp., *Sagitarria* sp., and *Hydropiper* sp.

Undisturbed sediment cores, along with overlying surface water (when present), were obtained from three substations at Eagle Island on a monthly basis (Figure 3). The first substation was located in the intertidal mud flat (I) region of the site and was within 1 meter of the marsh edge. The second substation was located in the marsh (M) and coincides with P6 substation 2 of the WHMP. The final substation was located along the edge between the marsh and upland transition zone (U) and coincides with P6 substation 6 of the WHMP.

Field Sampling

Sediment was collected during low tide using acrylic cores with dimensions 3 mm thick x 14.5 cm diameter x 25 cm long. One core was collected from each substation on successive months for a total of one calendar year (March 2006 through February 2007). Cores were sealed

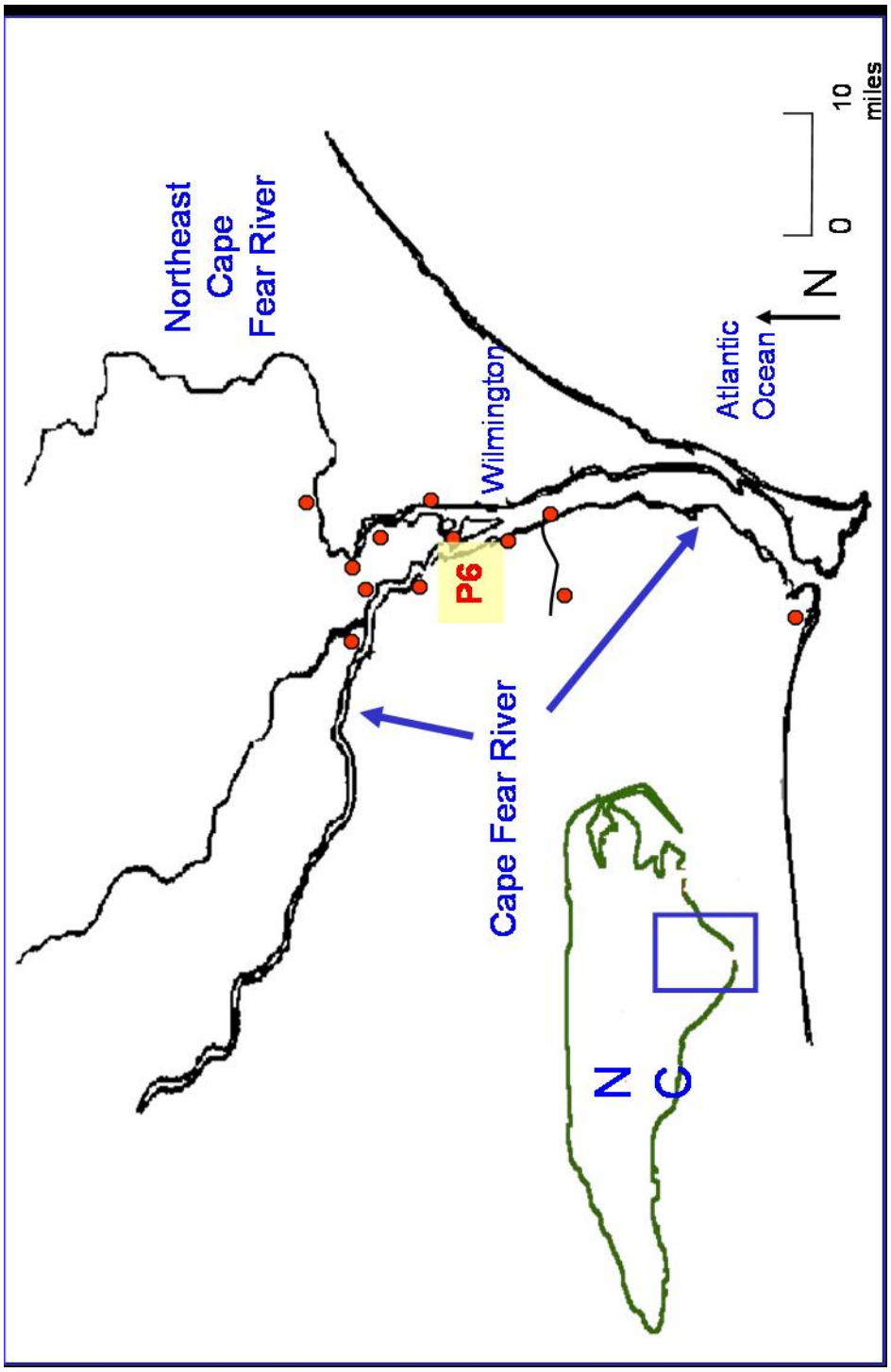

Figure 2. The Cape Fear River area including the Wilmington Harbor Monitoring Program study sites (Hackney et al., 2006). The three substations studied in this project are located at the Eagle Island (P6) station.

Figure 3. Aerial view of Eagle Island (P6) station, including the three substations used in this study; marsh/upland edge (U), marsh (M), and intertidal mud flat (I) substations (image obtained from Google Earth).

on the top and bottom with polyethylene caps and externally sealed with rubber gaskets on the bottom to prevent porewater leakage during transport. Due to time limitations, the cores were stored overnight under similar environmental conditions for profiling and analysis the following day. After electrode profiling was completed, the upper 3 to 4 cm of each core were collected and frozen for further solid phase metal analysis.

Electrode Polishing and Plating

The initial electrodes used in this study were provided by George Luther's laboratory located at the University of Delaware. Subsequently Au/Hg electrodes were assembled in our laboratory followed procedures outlined in Brendel (1995). After construction, the surface of the electrode was initially polished using 400 grit sandpaper to remove all major scratches and to provide an even electrode surface. A series of diamond polishes (15, 6, 1, and 0.05 μm) in succession were then used to obtain a mirror finish on the electrode surface. To check that the surface was flat and smooth, the tips of the electrodes were examined with a handheld microscope at a power of 100X.

Once an adequate surface was confirmed, the electrode was plated with Hg. The polished electrode and a saturated calomel electrode were placed in a 0.1 M ACS grade $Hg(NO_3)_2 \cdot H_2O$ (Baker) solution acidified to a pH of 1.5 with nitric acid that had been purged with nitrogen for 5 minutes. The plate was formed by electroreducing Hg(II) at a potential of -0.1 V for 4 minutes. The amalgam was then polarized to ensure reproducible peak positions and sensitivities necessary for analysis. This was accomplished by attaching the Au/Hg electrode to the negative terminal and a Pt wire to the positive terminal of a 9V battery, and placing them both in 1 M

NaOH solution for 90 seconds. Allowing the amalgam to set overnight reduced the electrical noise of the scans.

Electrode Calibration

Prior to electrode measurements, calibration curves for Fe^{2+}, Mn^{2+}, and HS^- were obtained using standard solutions as outlined by Brendel (1995) and Brendel and Luther (1998). Analytical grade chemicals $Fe(NH_4)_2(SO_4)2{\cdot}6H_2O$ (EM Science), $MnSO_4{\cdot}H_2O$ (Fisher), Na_2S (Aldrich), and MilliQ water were used to make standard solutions. To keep the redox species in reduced form, Mn and Fe standards were acidified to pH 2 with HCl. All calibrations were performed using 0.45 μm filtered Wrightsville Beach seawater as a supporting electrolyte. Deionized water was used to dilute the seawater when salinities under 32 were required. N_2 gas was bubbled through the seawater for 30 minutes prior to calibration to purge the water of O_2; bubbling was continued through analysis. Detection limits were determined for all analytes. Mn^{2+} was detected at concentrations above 20 μM, Fe^{2+} was detected at concentrations above 45 μM, and HS^- could be detected above 7 μM.

Additional treatments were required for Fe^{2+} standard curves since it tended to precipitate out of solution. To prepare Fe^{2+} calibration curves, seawater pH was adjusted to a range of 3 to 3.98 by adding HCl. Acetate buffer (0.1 M, pH 4.25) was added to stabilize the pH at this range. Additionally, any Fe^{3+} was reduced to soluble Fe^{2+} by adding analytical grade sodium dithionite (Aldrich) to the seawater to produce a 2.0 mM concentration solution. N_2 gas was bubbled continuously throughout scanning to maintain anoxic conditions.

The polarographic peak for sulfide is characterized as HS^-, which represents the sum of the H_2S, HS^-, and polysulfide species (Luther et al., 1998). Under the standard scanning

parameters used in this study (further described in the Methods section under Analytical Techniques), the total sulfide peak begins to split into two distinct peaks at concentrations above 100 μM. Calibrations were performed for concentrations below this point, and we extrapolated for higher concentrations.

Oxygen concentrations were determined in most cores using a Unisense OX100 microsensor. Microsensors were calibrated using manufacturer's instructions with Cape Fear River water collected from the field site on the same day as the cores, and at similar environmental temperatures. Nitrogen gas was bubbled through the river water for at least 10 minutes to remove O_2, and an aquarium pump was used to achieve O_2 saturation for calibrations.

Analytical Techniques

Each sediment core was analyzed using the voltammetric microelectrode system described in Brendel and Luther (1995). A standard three-electrode configuration, consisting of the Au/Hg working electrode, a saturated calomel reference electrode with salt bridge filled with saturated KCl, and a Pt wire counter electrode, was used in obtaining all electrochemical measurements. The reference and counter electrodes were inserted in the surface of the core approximately 1 to 2 cm from the entry point of the working electrode. The Au/Hg electrode was inserted into the sediment core using a micromanipulator. All voltammetric scans for Mn^{2+}, Fe^{2+}, and HS^- were performed using an Analytical Instrument Systems DLK-60 potentiostat using accompanying AIS software loaded onto a laptop. The potentiostat, cables, and laptop were electrically grounded to a copper water pipe and the system was powered by a 12 V marine battery in order to decrease external electrical noise.

The voltammetric technique used in this study was square wave voltammetry (SWV), where the waveform consists of a symmetrical square wave superimposed upon a staircase (Kounaves, 1997). The resultant net current of a redox reaction is the difference between the forward and reverse currents. Peak height is directly proportional to the concentration of the electroactive species reduced or oxidized at the working electrode. This method is ideal because it has the ability for low detection limits, fast scan rates, and exclusion of background noise (Brett and Brett, 1998).

Standard parameters used for SWV were as follows: pulse height 15 mV, step increment 2 mV, frequency 100 Hz, scan rate 200 mV sec^{-1}. The voltage range scanned was generally from -0.1 to -1.8 V. As described in Brendel and Luther (1995), the microelectrode is conditioned at each scan by applying a potential that removes any previously deposited redox-active species. For the purpose of this study, the potential applied was -0.8 V for 2 min to oxidize any HgS that forms in the presence of sulfide species. After conditioning, the electrode was allowed to equilibrate for 5 s before applying the wave form.

Prior to taking measurements in the cores, the electrode was calibrated for Mn under the same environmental conditions (salinity and temperature) in which the cores were collected. Seawater was diluted with deionized water for lower salinity calibrations and placed in an ice bath to reach environmental temperatures where needed. Because calibrations were previously generated for all analytes (Mn^{2+}, Fe^{2+}, and HS^{-}) we used the "pilot ion method" (Meites, 1965) to obtain calibration curves for all analytes on a given day since the relative slopes for these curves are constant. Mn was chosen as our standard for calibration because it is most stable at seawater pH.

After calibration measurements were then obtained from the sediment cores. Each core was sectioned into 4 quadrants, using two for voltammetric analysis and two for O_2 profiling. For each profile, the working electrode was placed in the center of the quadrant so that it was away from the side of the core tube and from locations where subsequent profiles would be obtained. Voltammetric measurements were taken over a total depth of 6 to 10 cm, depending on the amount of root and rhizome material in the sediments. Oxygen measurements were taken over a total depth of 3 to 5 cm, although O_2 was typically only within the surface 1 cm. Generally, two depth profiles for both the Au/Hg microelectrode and O_2 microsensor were generated in each core. After the completion of all microelectrode analysis, approximately 5 cm of surface sediment was collected and frozen for Fe and Mn analysis.

Data collected with the DLK-60 software were transferred into Excel spreadsheets and imported to the program PeakFit (Jandel Scientific) for peak height measurements. This software is useful for measuring accurate baselines and obtaining high resolution for all analytes studied, but especially for Fe when Mn is present (Brendel, 1995). Where more than one analyte was present, seperate baselines were drawn and each peak was calculated independently of the others (Figure 4).

Solid Phase Metal Sampling

Reactive solid phase Mn and Fe were determined for sediment samples from July 2006 through February 2007 using dithionite extraction methods described by Kostka and Luther (1994). Prior to analysis, frozen sediment samples from each of the cores collected were thawed and homogenized with a plastic spatula. Triplicate 0.5 to 1.0 g samples were placed into pre-

weighed aluminum pans and dried at 60 °C until a constant mass was reached for calculation of wet-dry weight ratios.

Triplicate 0.4 to 0.6 g wet sediment samples were placed into 15 ml centrifuge tubes containing 0.5 g sodium dithionite in 10 ml of 0.35 M acetate/0.2 M sodium citrate (pH 4.8). These samples were placed onto a water bath rotary shaker at 60 °C and at a speed sufficient to maintain constant suspension for 4 hours. Supernatants were removed and analyzed on a Perkin Elmer Atomic Absorption Spectrometer Model 3110. Concentrations of dithionite-reactive Fe and Mn were determined using matrix-matched standard curves.

Organic Content Analysis

Percent organic carbon was determined for sediment samples from July 2006 through February 2007, and from all three substations (substation U sediments began in September 2006) by combustion. Frozen sediment samples from each of the cores collected were thawed and homogenized with a plastic spatula, and dried overnight at 60 °C. Triplicate 0.5 g dry sediment samples were weighed and placed into pre-weighed aluminum pans and combusted overnight at 450 °C. Samples were reweighed after cooling in a desiccator.

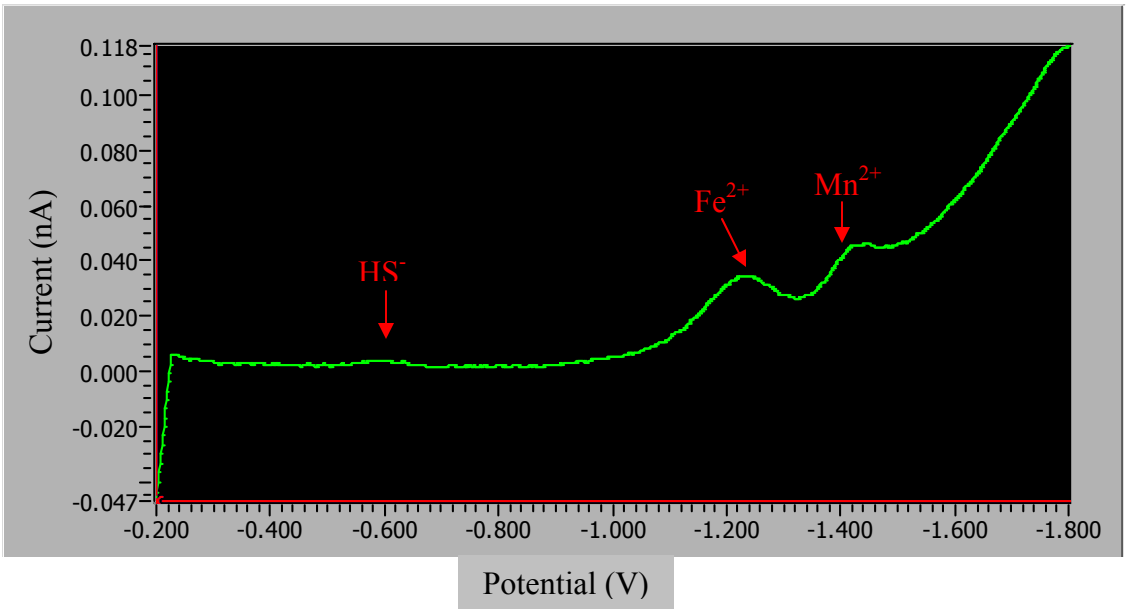

Figure 4. Voltammetric scan with potential (V) on the x-axis and current (nA) on the y-axis; peaks for Mn^{2+} at -1.43 V, Fe^{2+} at -1.23 V, and HS^- beginning to show a peak at -0.6 V.

RESULTS AND DISCUSSION

Physical and Chemical Characterization of Substations

River flow and precipitation data for the Cape Fear River was obtained for the duration of the study period from the USGS National Water Information System, Cape Fear River Lock #1 data set (http://waterdata.usgs.gov/nc/nwis; Table 2). These data represent values for the seven days prior to and including core collection sampling days. Average monthly river flow varied throughout the sampling period from 26 $m^3 s^{-1}$ to 393 $m^3 s^{-1}$. Peaks in flow were observed during November and January, whereas low flow occurred in June. Monthly rainfall totals during the sampling year varied from 0 cm to 5.52 cm. Peaks in rainfall occurred during August, September, and November.

Intertidal Mud Flat

Sediment collected from the intertidal mud flat (substation I) was a uniform charcoal gray color, and was composed of fine grain size particles (visual inspection, actual grain size was not measured). This sampling substation lacked vegetation (including roots and rhizomes) throughout the year. With the exception of a few tube dwelling worms, cores from this site lacked visible infauna. Additionally, there were few or no air pockets resulting in relatively uniform consistency and compaction. Sediment pH was measured during December through February, and ranged from 5.4 to 6.3.

Reactive solid phase Mn and Fe, percent water content, and percent organic carbon were determined for sediment cores collected from July 2006 through February 2007 (Table 3). Reactive Fe varied from 22 (±2) μmol g^{-1} to 169 (±20) μmol g^{-1} and reactive Mn varied between

Table 2. River flow and rainfall data for the Cape Fear River prior to data collection.

Month	7 Day Ave River flow (m^3/s)	7 Day Total Rainfall (cm)
March 2006	59 ± 5	0.28
April 2006	32 ± 3	0.00
May 2006	59 ± 10	1.73
June 2006	26 ± 4	4.55
July 2006	131 ± 68	0.00
August 2006	45 ± 6	5.33
September 2006	75 ± 18	5.45
October 2006	36 ± 6	2.95
November 2006	342 ± 78	14.0
December 2006	169 ± 91	0.00
January 2007	393 ± 77	2.95
February 2007	179 ± 26	0.00

Data averaged for 7 days prior to and including the core sampling day from the USGS National Water Information System, Cape Fear River Lock #1 data set (http://waterdata.usgs.gov/nc/nwis). The 7 day average river flow and total rainfall were calculated from these data.

the months with a range of 0.2 (±0.03) μmol g^{-1} to 4.6 (±0.2) μmol g^{-1}. These values are considerably lower than the other two sampling substations (Tables 3, 4, and 5). Values of reactive Mn have been found to range between 1 and 18 μmol g^{-1} in coastal marine sediments in Denmark (Thamdrup et al., 1994) and <0.5 μmol g^{-1} in coastal sediments off Corpus Christi, TX (Sell, 2003). Reported values for reactive Fe have ranged from between 2.62 and 200 μmol g^{-1} in coastal marine sediments (Sell, 2003; Thamdrup et al., 1994), and 450 μmol g^{-1} in salt marsh sediments (Kostka and Luther, 1994). The ranges of values for reactive solid phase Mn and Fe observed in this study fall within the range observed in coastal marine sediments rather than a salt marsh systems.

Average percent organic carbon content at this site was 16 (±3), with a minor peak observed at the end of summer. This annual average is considerably lower than the other two substations in this study, and can be attributed to the lack of vegetation in the intertidal zone. Average percent water content was 66 (±12), which is also the lowest value out of the three substations.

Salinity at substation I during the sampling year was highly variable, ranging from and <0.1 to about 5, and showing no discernible trends or patterns (Table 3). Porewater salinity values were obtained from WHMP, site P6, S1-1 (Hackney et al., 2006; Hackney et al., 2007). Although this substation is located in the vegetated section of the marsh, it is the closest sampling substation to the channel bank of the river monitoring project, and consequently to this study's substation I. Peaks in salinity were observed during April, June, and October. These peaks were not followed by a slow steady decrease but often displayed dramatic decreases the next month. Dramatic changes in salinities are most likely due to variations in river stage and

rainfall, and suggest that the porewaters are reflecting the rapid changes seen in the overlying water.

Marsh

Sediments in the marsh (substation M) were generally dark brown in color. Consistent with previous findings in similar systems (e.g. Valiela et al., 1976), the upper 5 cm to 15 cm contained dense root and rhizome material (visual observation). The amount of root and rhizome material varied throughout the sampling year, but was present even during the winter when there was little or no aboveground biomass. Fiddler crabs were commonly observed in this area of the marsh, and were often collected in the cores. Additionally, there were often gas filled spaces within the sediment that were visible through the side of the core. Sediment pH was measured December through February and ranged from 5.8 to 6.7.

Reactive solid phase Mn and Fe, percent water content, and percent organic carbon were obtained for sediment cores collected from July 2006 through February 2007 (Table 4). Reactive Fe varied from 41 (±5) μmol g^{-1} to 96 (±9) μmol g^{-1} and reactive Mn varied with a range of 2.3 (±0.1) μmol g^{-1} to 5.7 (±0.7) μmol g^{-1}. As seen in the intertidal mud flat substation, reactive Fe and Mn values in the marsh were consistent with those observed in coastal marine sediments (Sell, 2003; Thamdrup et al., 1994), and much lower than the Fe content described in salt marsh sediments (Kostka and Luther, 1994). Additionally, the reactive Mn content was consistently higher in the marsh sediments than in the other two substations (Tables 3, 4, and 5). Average percent organic carbon content at this site was 52 (± 10) and the average percent water content was 88 (±4). A peak in the organic carbon content was observed in the end of summer.

Table 3. Chemical and physical characterization of substation I.

	Mar-06	Apr-06	May-06	Jun-06	Jul-06	Aug-06	Sept-06	Oct-06	Nov-06	Dec-06	Jan-07	Feb-07	Mean
% OC	n/a	n/a	n/a	n/a	17	17	17	19	16	13	12	14	16 ± 3
% H_2O	n/a	n/a	n/a	n/a	63	49	65	72	89	64	58	62	66 ± 12
R-Fe (µmol/g dwt)	n/a	n/a	n/a	n/a	145 ± 100	169.± 20	30 ± 2	36 ± 1	22 ± 2	53 ± 0.8	26 ± 2	23 ± 1	56.0 ± 59.3
R-Mn (µmol/g dwt)	n/a	n/a	n/a	n/a	2.5 ± 0.2	1.4 ± 0.1	0.9 ± 0.1	0.2 ± 0.03	2.9 ± 0.2	4.6 ± 0.2	0.9 ± 0.3	1.2 ± 0.06	1.6 ± 1.5
Salinity	2.2	5.0	0.2	5.0	0.03	1.8	0.4	4.3	0.07	1.6	0.09	1.6	1.9 ± 1.9

Organic carbon (% OC), water content (% H_20), reactive solid phase iron (R-Fe), and reactive solid phase manganese (R-Mn) determined for sediment samples from July 2006-February 2007. n/a = No data collected. Salinity data are from site P6, S1-1 of the WHMP (Hackney et al., 2006; Hackney et al., 2007).

Table 4. Chemical and physical characteristics of substation M.

	Mar-06	Apr-06	May-06	Jun-06	Jul-06	Aug-06	Sept-06	Oct-06	Nov-06	Dec-06	Jan-07	Feb-07	Mean
% OC	n/a	n/a	n/a	n/a	37	48	68	57	44	53	57	56	52 ± 10
% H_2O	n/a	n/a	n/a	n/a	79	84	89	89	90	90	89	91	88 ± 4
R-Fe (µmol/g dwt)	n/a	n/a	n/a	n/a	77 ± 7	60 ± 12	41 ± 5	58 ± 5	96 ± 9	47 ± 3	49.2	57 ± 5	63 ± 28
R-Mn (µmol/g dwt)	n/a	n/a	n/a	n/a	2.9 ± 0.5	3.3 ± 0.3	2.3 ± 0.1	3.6 ± 0.4	3.6 ± 0.4	5.7 ± 0.7	2.8	5.0 ± 0.9	3.2 ± 1.6
Salinity	2	6.24	0.51	5.92	1.67	2.54	0.5	2.08	0.31	0.94	2.26	1.04	2.17 ± 1.97

Organic carbon (% OC), water content (% H20), reactive solid phase iron (R-Fe), and reactive solid phase manganese (R-Mn) determined for sediment samples from July 2006-February 2007. n/a = No data collected. Salinity data are from P6 (S2) of the WHMP (Hackney et al., 2006; Hackney et al., 2007).

Table 5. Chemical and physical characteristics of substation U.

	Mar-06	Apr-06	May-06	Jun-06	Jul-06	Aug-06	Sept-06	Oct-06	Nov-06	Dec-06	Jan-07	Feb-07	Mean
% OC	n/a	n/a	n/a	n/a	n/a	n/a	69	72	74	73	75	71	72 ± 2
% H_2O	n/a	n/a	n/a	n/a	n/a	n/a	89	89	60	90	90	90	85 ± 12
R-Fe (µmol/g dwt)	n/a	n/a	n/a	n/a	n/a	n/a	62 ± 7	80 ± 16	23 ± 4	113 ± 1	86 ± 65	181 ± 9	78 ± 59
R-Mn (µmol/g dwt)	n/a	n/a	n/a	n/a	n/a	n/a	2.9 ± 0.2	1.7 ± 0.08	1.3 ± 0.2	4.2 ± 0.4	2.9 ± 1.8	3.6 ± 0.1	2.3 ± 1.4
Salinity	0.43	1.44	0.47	1.11	0.17	0.53	1.82	0.85	0.19	0.27	0.24	0.19	0.64 ± 0.55

Organic carbon (% OC), water content (% H20), reactive solid phase iron (R-Fe), and reactive solid phase manganese (R-Mn) determined for upland sediment samples from September 2006-February 2007. n/a = No data collected. Salinity data are from P6 (S6) of the WHMP (Hackney et al., 2006; Hackney et al., 2007).

Salinity input to substation M during the sampling year was highly variable and were similar to values measured at substation I (Tables 3 and 4). Reported salinity values were obtained from WHMP, site P6, S2-1 (Hackney et al., 2006; Hackney et al., 2007), and ranged from 0.31 to 6.2. Peaks in salinity were observed during April and June. As observed in substation I, there was a dramatic decrease in salinity during the months following these peaks rather than a slow steady decrease. Due to higher percentages of water content, the less compacted nature of the sediments, and the presence of vegetation at this substation, salinity variations could be attributed to rapid porewater flushing, a groundwater effect, or rapid changes in river salinities being reflected in interstitial waters.

Marsh/Upland Edge

Sediments collected from the marsh/upland edge (substation U) were dark brown in color; however an orange-rust color ooze often seeped out of the sediments during core extraction, characteristic of Fe oxyhydroxides. As at substation M, roots and rhizomes were present throughout the year even when there was little or no aboveground biomass. In addition to the root mat, however, substation U often contained larger root structures which penetrated deeper into the sediment. Fiddler crabs were often found in the cores, and on one occasion a larval fish was present in the overlying water of the core. Gas filled spaces within the sediment were visible through the side of the core, similar to those observed at substation M. Sediment pH was measured during December through February, and ranged from 5.7 to 6.5.

Reactive solid phase Mn and Fe, percent water content, and percent organic carbon were obtained for sediment cores collected from September 2006 through February 2007 (Table 5). Coinciding with the observed Fe oxyhydroxides, reactive Fe was highest at this substation varying from 23 (±4) μmol g^{-1} to 181 (±9) μmol g^{-1}, but was still consistent with the range

described in coastal marine sediments (Sell, 2003; Thamdrup et al., 1994). Reactive Mn varied between months with a range of 1.3 (± 0.2) μmol g^{-1} and 4.2 (±0.4) μmol g^{-1}. Percent organic carbon content at this substation was the highest out the three with a mean value of 72 (±2). Average percent water content was 85 (±12), the highest of all the substations.

Salinity at substation U during the sampling year was lower and varied less than at the other two sampling sites (Table 5), consistent with a further distance of this substation from the river channel and therefore more influence from upland groundwater and runoff. Salinity values were obtained from WHMP, site P6, S6-1 (Hackney et al., 2006; Hackney et al., 2007) and ranged from 0.17 to 1.82. Peaks in salinity were observed during April, June and September, consistent with modest river flows during these months (Table 4). Although these peaks were smaller than in the other two study sites, they did not decrease slowly and often displayed similar dramatic decreases the next month.

Biogeochemical Processes

Oxygen

O_2 was measured with the Unisense OX100 microsensor in all cores from the months of July 2006 through February 2007, excluding September 2006 when the instrument was broken (Figures 5, 6, and 7). O_2 was present in substation I cores (Figure 5) from all months sampled, except in October and December of 2006 when no O_2 was detected. Concentrations in the overlying water ranged from 86 μM to 312 μM, and from 0 μM to 254 μM in the sediments. Depletion occurred within 4 to 6 mm below the sediment-water interface. The deepest detectable O_2 (3.5 μM) occurred in February 2007 at a depth of 6 mm.

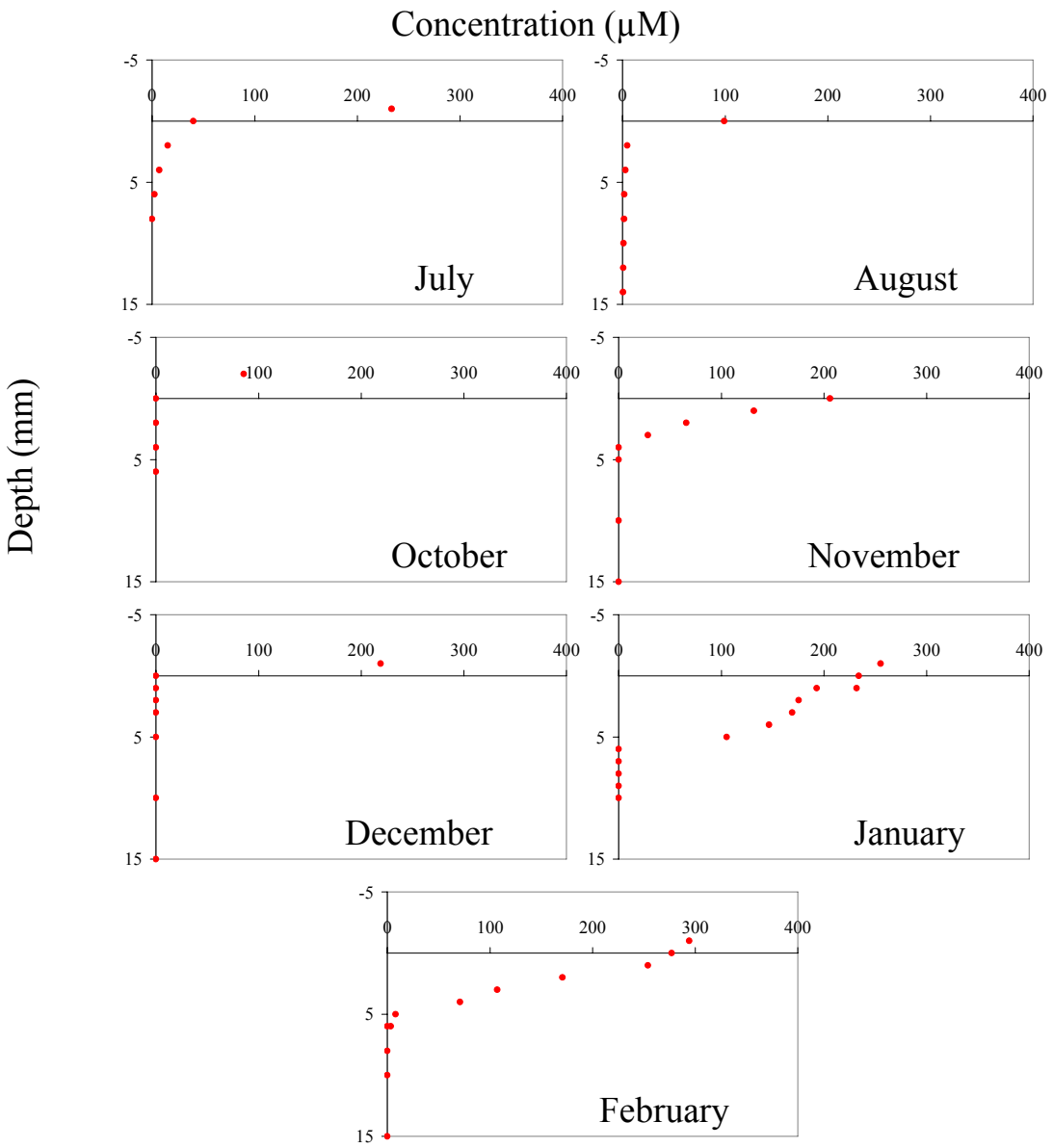

Figure 5. Intertidal mud flat (I) substation O_2 depth profiles.

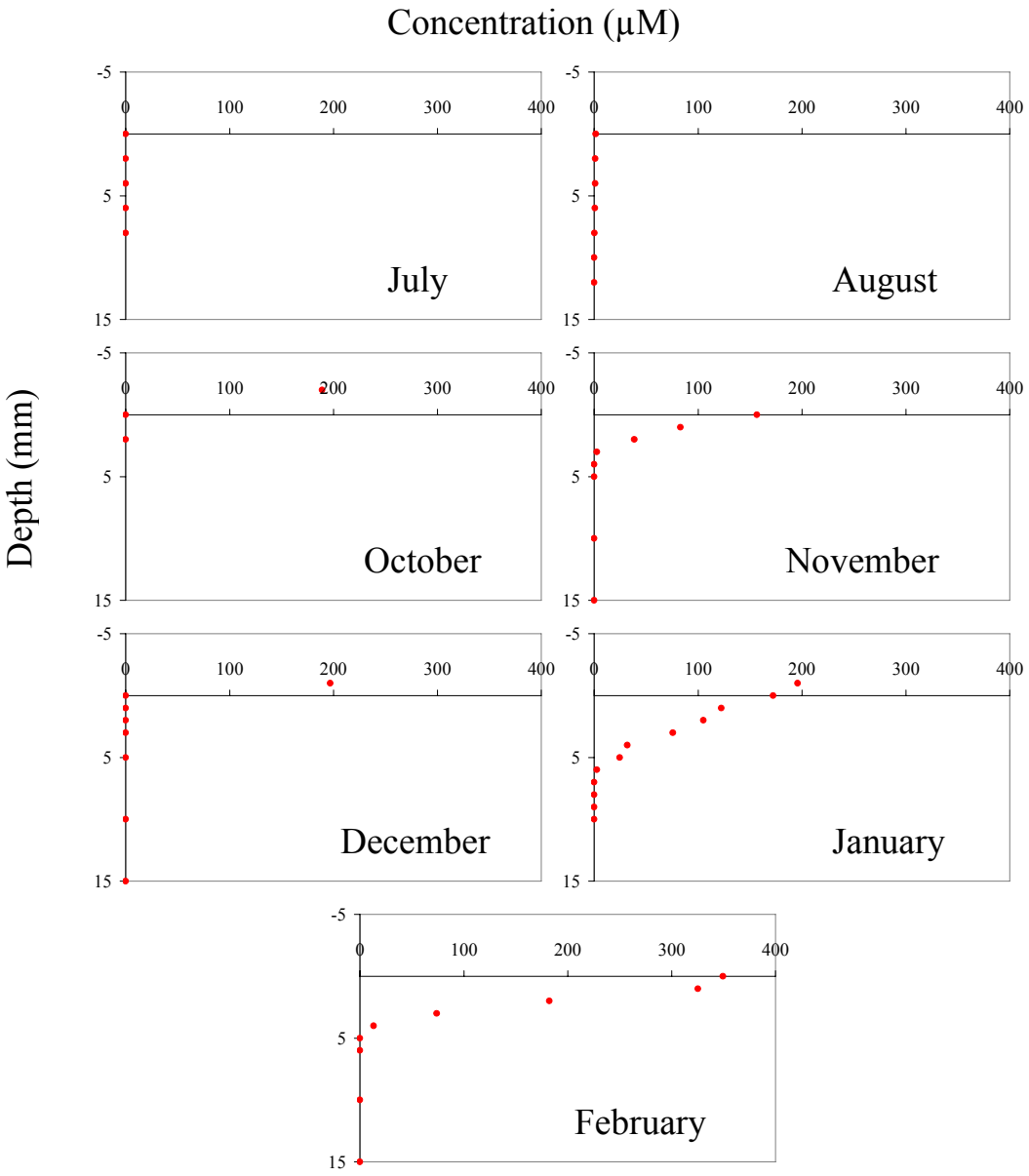

Figure 6. Marsh (M) substation O_2 depth profiles.

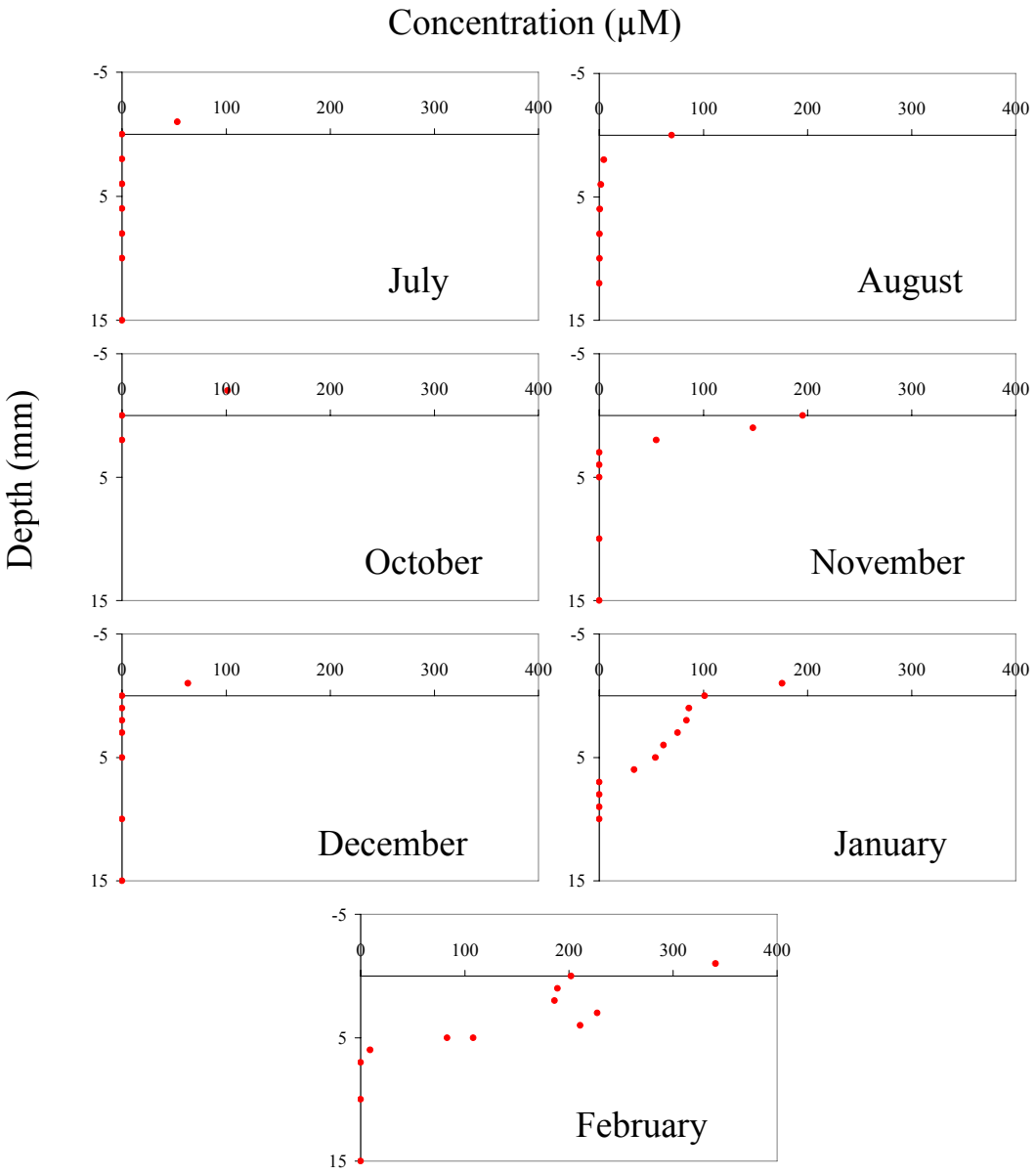

Figure 7. Marsh/upland edge (U) substation O_2 depth profiles.

O_2 was detected in substation M cores (Figure 6) during the months of November, January, and February. Concentrations in the overlying water ranged from 137 μM to 243 μM, and from 0 μM to 349 μM in the sediments. O_2 was detected during the same months in substation U cores (Figure 7), with the addition of August. Concentrations in the overlying water ranged from 42 μM to 341 μM, and from 0 μM to 227 μM in the sediments. In both substations, O_2 was depleted by depths between 3 and 7 mm. An overall trend emerged in both M and U substations, where the presence of oxygen occurred in the surface sediments during the non-growing season (winter) and was absent during the growing season (summer). Studies examining root zones in salt marsh sediments have shown a seasonal oxygen supply via roots sufficient to oxidize the pool of reduced sediment components, with the presence of oxygen noted at depths >20 cm (Sundby et al., 2003; Koretsky et al., 2000). Since O_2 was not detected in the root zones of substations M and U in this study, it is assumed that O_2 diffusion from the sediment-water interface and flux from the roots was insufficient to overcome local demand for oxygen by reduced sediment components. The presence of O_2 during winter could be attributed to increased O_2 solubility and/or slower aerobic respiration rates at lower temperatures.

Suboxic and Anoxic Processes

Methane concentrations, sulfate concentrations, and chloride to sulfate ratios were obtained for the surface 6 cm of sediment from the corresponding WHMP substations (Figures 8, 9, and 10). Methane was detected at all three substations, with consistently high values in the upland which decreased across the landscape of the marsh toward the channel bank (Figure 8). Sulfate concentrations ranged from 32 μM to 4000 μM (Figure 9). Previous published values for sulfate concentrations sufficient to support active SR have ranged from 20 μM (Sexton, 2002) to 200

μM (Hoehler, 1998). Sulfate concentrations were greatest in intertidal mud flat sediments, followed by the marsh, and were lowest in marsh/upland edge sediments. Chloride to sulfate ratios reflect patterns of sulfate consumption throughout the sampling period. Chloride and sulfate concentrations have a constant molar ratio in typical oxygenated seawater (19.3:1). Unlike sulfate, which can decrease due to sulfate reduction, there are no common removal mechanisms (biotic or abiotic) for chloride from seawater. Therefore, changes in the ratio of chloride to sulfate ratios are an indicator of sulfate reduction or sulfide oxidation. The ratios from this study period range from those found in seawater to higher ratios indicating a depletion of sulfate due to sulfate reduction (Figure 10). Lower ratios also occurred, a possible indication of H_2S oxidation from previous sulfate reduction.

Detailed depth profiles obtained with the microelectrode (Figures 11-22) indicate small-scale heterogeneity within substations. Additionally, a high level of variability was observed across the landscape of the study site, suggesting that remineralization processes differ between substations. August was unique in that the concentrations of all dissolved analytes (Mn^{2+}, Fe^{2+}, and HS^-) were at or below detection limits for all the profiles from each substation (Figure 16). Warm temperatures and peak plant biomass suggest evapotranspiration could be occurring at high levels. Evapotranspiration can be significant in the vertical flux of interstitial water from marsh sediments (Odum, 1988). Replacement of sediment porewaters can occur via vertical infiltration of flooding tidal water and rainfall (Yelverton and Hackney, 1986; Odum, 1988), or upland groundwater flow (Carr and Blackley, 1986; Valiela et al., 1986). Results of this study suggest that the combined effects of elevated evapotranspiration, high rainfall during the week leading up to field sampling (5.33 cm), and low river flow (45.1 ± 5.9 m^3 s^{-1}) resulted in hydrological "flushing" of the porewaters during August. Incoming water would reoxidize

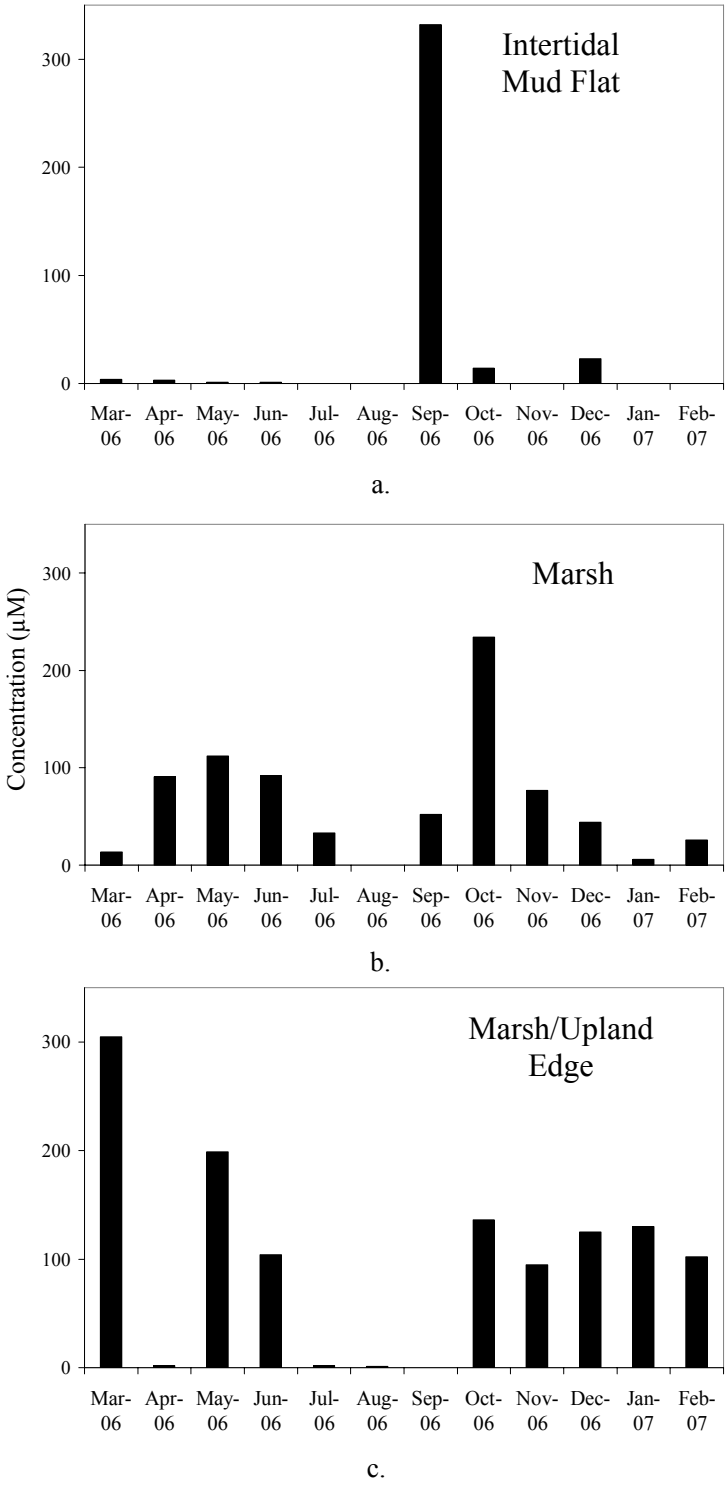

Figure 8. Methane concentrations of three Eagle Island substation porewaters vs. month March 2006-February 2007. Data obtained from Hackney et al., 2006 and Hackney et al., 2007.

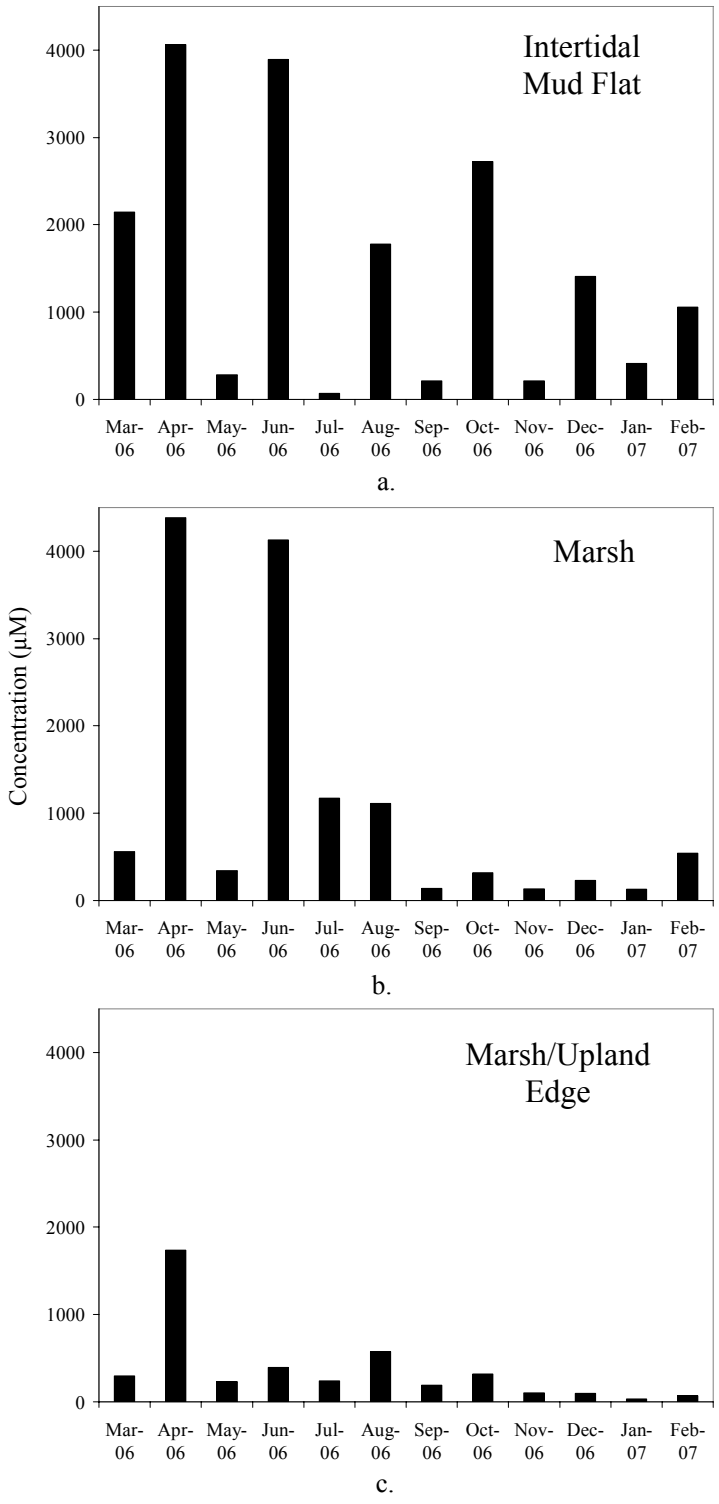

Figure 9. Sulfate concentrations of three Eagle Island substation porewaters vs. month March 2006-February 2007. Data obtained from Hackney et al., 2006 and Hackney et al., 2007.

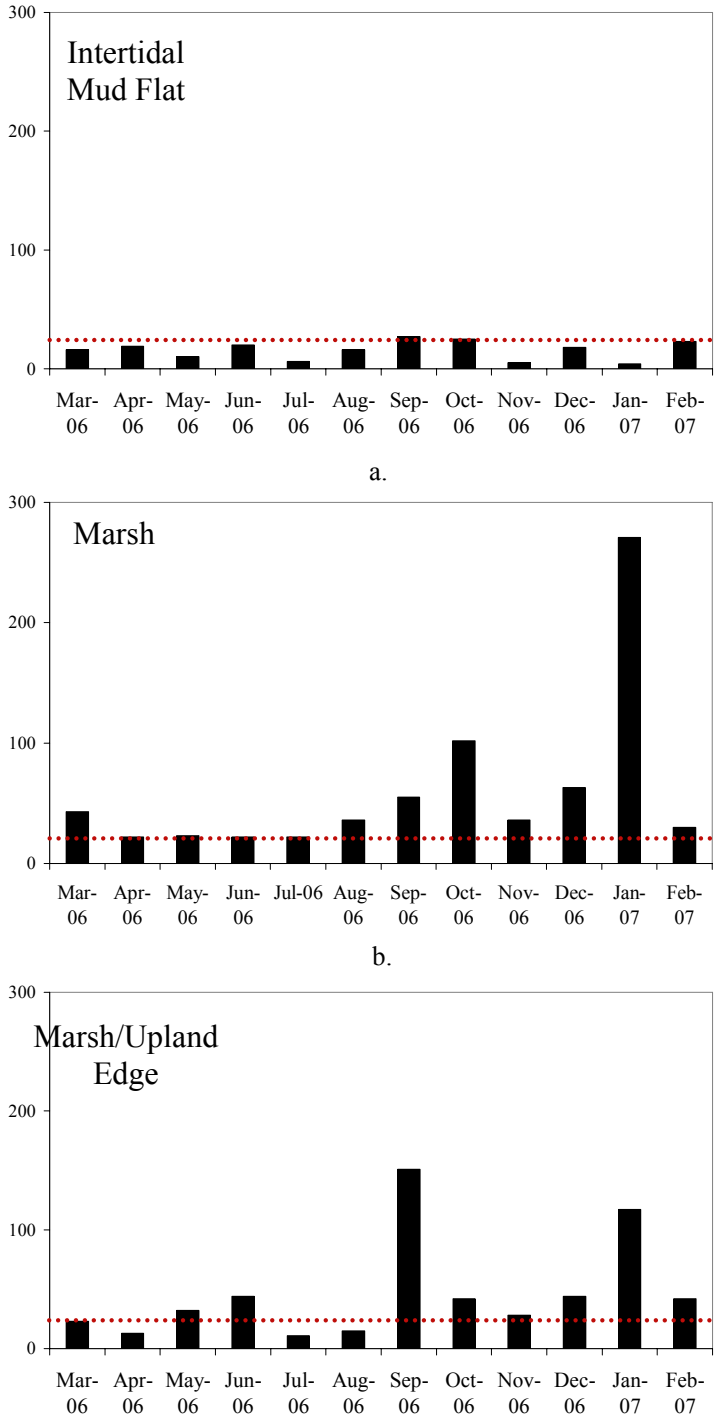

Figure 10. Chloride to sulfate ratios of three Eagle Island substation porewaters vs. month March 2006-February 2007. Red dotted line represents seawater ratio (19.3:1). Data obtained from Hackney et al., 2006 and Hackney et al., 2007.

reduced species, using available O_2 and preventing the accumulation of Mn^{2+}, Fe^{2+}, and HS^- in sediment porewaters. Furthermore, the reoxidation of Fe^{2+} produces Fe(III) (hydr)oxide minerals (Mendelssohn and Postek, 1982; Sundby et al., 1998), which in turn reoxidize dissolved sulfide (Yao and Millero, 1996; Koretsky et al., 2003).

Substation Comparisons

Intertidal Mud Flat

Although no two depth profiles were entirely identical, cores from substation I were relatively homogeneous during most sampling months. Despite differences in concentrations, the vertical succession of analytes with depth was similar within the cores collected during April (Figures 12a and 12b), June (Figures 14a and 14b), August (Figures 16a and 16b), September (Figures 17a and17b), December (Figures 20a and 20b), January (Figures 21a and 21b), and February (Figures 22a and 22b). Only one profile was collected during March, so variations within the core cannot be determined. April and December profiles were dominated by dissolved Mn through the entire depth of the profiles; no other analytes were detected during these months. August and February cores exhibited analyte concentrations that were at or below the detection limits for all dissolved species. Large concentrations (~475 μM) of Fe^{2+} were measured in the surface sediments of the January profiles and declined between 0.5 and 2.5 cm. When Fe^{2+} tapered off, Mn^{2+} appeared, but remained in low concentrations (<40 μM). June profiles showed Mn^{2+} in the surface sediments, followed by a steady increase of HS^- as Mn^{2+} began to decrease. The remainder of the sampling months exhibited small-scale variation in the profiles.

Higher salinities (≥5) were measured closest to the channel bank (Table 3), resulting in an inhibition of methanogenesis at substation I. Consequently, methane concentrations at this substation were lower in comparison to the other two substations in this study (Figures 8a, 8b, and 8c). Although there was a peak in methane (>300 μM) production observed during the September sampling period (Figure 8a), the intertidal region of this site does not appear to be dominated by methanogenesis.

Sulfate concentrations in the upper 6 cm of sediment in substation I ranged from 70 μM to >4000 μM (Figure 9a), above the threshold values for sulfate reduction (Sexton, 2002; Hoehler, 1998). Consistent chloride to sulfate ratios at or below that of seawater (Figure 10a) offer further evidence that SR occurs in substation I. However, the general absence of dissolved sulfide in the vertical profiles indicates that either SR may be occurring at low levels, that sulfide is being oxidized by Fe and Mn hydroxides, or that the products of SR are being precipitated. Low levels of SR might suggest that more thermodynamically favored processes are responsible for the remineralization that is occurring in the surface sediments of the intertidal region. If sufficient levels of Mn and Fe reduction are occurring, these processes could be driving SR to depths deeper than examined in this study (Roden and Wetzel, 1996). Mn^{2+} was detected more consistently and in higher concentrations than Fe^{2+}, indicating that Mn reduction plays an important role in remineralizing the organic matter in the intertidal surface sediments.

If SR is occurring in the presence of reduced Fe, HS^- produced is rapidly consumed and maintained at low concentrations such that any available Fe^{2+} is rapidly bound in FeS (Howarth, 1984; Swider and Mackin, 1989). This process pulls Fe^{2+} and HS^- out of porewater, and inhibits the detection with the Au/Hg microelectrode. When Fe is bound in mineral forms, including FeS and FeS_2, Mn reduction may become more important (Joye et al., 1996). The equilibrium

between the dissolved and solid phases of FeS compounds can be a major factor in the uptake and release of both Fe^{2+} and HS^-. If the solubility product for FeS is exceeded, it will form FeS_2 and precipitate and subsequently reduce the voltammetric signal for Fe^{2+} (Taillifert et al., 2000).

In porewater, the concentrations of Fe^{2+} and HS^- can be controlled by the solubility of mackinawite, a common iron sulfide mineral in sediments. When dissolved Fe^{2+} and HS^- are present and detectable in a microelectrode scan, the saturation state of the porewaters with respect to mackinawite can be determined (Equations 1-8; Sell, 2003). This calculation will determine if aqueous FeS is likely to precipitate out of a system completely. The presence of aqueous FeS can be detected, but not quantified, with the Au/Hg microlelectrode. The characteristic peak for this compound is a broad peak occurring around -1.1 V (Theberge and Luther, 1997).

(1) $$\alpha_{Fe^{2+}} = \gamma_{Fe^{2+}} \cdot m_{Fe^{2+}}$$

(2) $$\alpha_{H^+} = \gamma_{H^+} \cdot m_{H^+}$$

(3) $$\sum H_2S = m_{H_2S} + m_{HS^-}$$

(4) $$K_1 = \frac{\left(\alpha_{HS^-} \cdot \alpha_{H^+}\right)}{\alpha_{H_2S}} = 10^{-6.9}$$

(5) $$K_{FeS(mack)} = \frac{\left(\alpha_{HS^-} \cdot \alpha_{Fe^{2+}}\right)}{\alpha_{H^+}} = 10^{-2.96}$$

(6) $$m_{HS^-} = \frac{K_1 \gamma_{H_2S} \sum H_2S}{\left(\gamma_{HS^-} \cdot \alpha_{H^+} + K_1 \cdot \gamma_{H_2S}\right)}$$

(7) $$\Omega = \frac{\left(\alpha_{HS^-} \cdot \alpha_{Fe^{2+}}\right)}{K_{FeS(mack)}} \cdot \alpha_{H^+}$$

Where α is the activity product, γ is the activity coefficient, *m* is the molality, *K* is the solubility product for mackinawite, K_1 is the dissociation constant for sulfide, and Ω is the saturation state with respect to mackinawite. The saturation states for FeS, with respect to mackinawite, were calculated (where appropriate) following the same parameters as Sell (2003) with the microelectrode measurements for Fe^{2+} and H^+ from this study. Although aqueous FeS was detected in intertidal mud flat cores during April (Figure 12a and 12b); May (Figure 13a and 13b); November (Figure 19a); and February (Figure 22b), Fe^{2+} and HS^- were undetectable and therefore the saturation state for solid FeS with respect to mackinawite could not be determined.

Physical characteristics of the intertidal region of Eagle Island influence porewater patterns of Mn^{2+}, Fe^{2+}, and HS^-. Remineralization reactions may be limited by a lack of labile organic matter supply (Table 3), relative to the vegetated marsh and upland areas in this study. O_2 was detected in the surface sediments during most months sampled, and Mn reduction appeared to dominate suboxic pathways, insinuating that these processes are consuming what organic matter is available. Furthermore, although organic matter was not characterized, it may be largely recalcitrant, and therefore less bioavailable for bacterial respiration (Alongi et al., 1998; Westrich and Berner, 1984).

Marsh

The large network of roots and rhizomes in the upper sections of the marsh sediments created difficulties in vertically manipulating the microelectrode, which often limited the depth of the profiles. Profile depths of at least 6 cm were attempted, and September was the only month in which the root mat resistance limited the depth of profiles to 5 cm and 2.5 cm in depth,

respectively (Figures 17c and 17d). Since HS^- was the only analyte detected at these depths, scans at further depths in this case may be inconsequential to the results of this study.

Although there were fine-scale variations in the depth profiles, a surprisingly high amount of overall homogeneity within cores was seen at this substation. Similar depth profile trends were observed within cores from all months except April (Figures 12c and 12d), June (Figures 14c and 14d), and July (Figures 15c and 15d). Only one profile was collected during March (Figure 11b), and technical complications in November (Figure 19c) resulted in a single profile, so variations within the cores could not be determined.

Months in which heterogeneity existed coincide with active plant growth, elucidating the influence of roots on the small-scale biogeochemical processes in sediments. Evapotranspiration, exudation of metabolic oxidants, and O_2 loss from plant roots greatly influence the oxidation-reduction chemistry of marsh sediments (e.g. Howes et al., 1984; Howes et al., 1981; Teal and Kanwisher, 1966; Sundby et al., 2003). Microzones within the rhizosphere can occur within 2 mm of one another (Sundby et al., 2003), creating a highly variable and heterogeneous chemical environment (Devries and Wang, 2003; Wang and Peverly, 1999). The role of vegetation is particularly evident in depth profiles from July. The first profile (Figure 15c) is dominated by reduced Mn and Fe, representing more oxidizing conditions near a root than the second profile (Figure 15d) in which HS^- dominates.

The depth profile from March (Figure 11b) did not follow the predicted biogeochemical zonation pattern. Sulfide was detected (~ 158 μM) at the surface and steadily decreased to undetectable levels around 1 cm. This section was primarily sediment, as it occurs above the rhizosphere and does not experience aeration by roots, allowing dissolved sulfide to accumulate.

As the profile intersects the rhizosphere, HS^- rapidly decreased and Mn^{2+} was detected (between 15 to 50 μM) throughout the rest of the profile.

Seasonal trends emerged from the marsh substation throughout the sampling period. Sulfate reduction appeared to dominate most of the remineralization during the growing season, with some contribution by Mn reduction in the surface 2 cm. From April through July, sulfate concentrations (Figure 9b) were far above the threshold required to sustain SR, and chloride to sulfate ratios (Figure 10b) were similar to those of seawater indicating an ample resupply of sulfate. Although reactive solid phase Mn was highest in marsh sediments (Tables 3, 4, and 5), bacterial Mn reduction may not be an important remineralization process during the summer months. Because sulfide was detected close to the surface, due to sulfate reducing bacteria thriving off root exudates (Mendelssohn et al., 1981; Hines et al., 1989), H_2S produced could reduce available Mn oxides. This chemical cycling can limit the availability of Mn oxides for bacterial reduction except near the sediment-water interface, where sulfate reduction is not occurring (Lovely and Phillips, 1988).

As the organic matter from the plants which drives SR is consumed, the dominant pathway for carbon remineralization in the marsh may shift from sulfate reducing to other anaerobic respiration mechanisms in the fall and winter. HS^- was no longer detected in November (Figure 19c), and did not begin to reappear through the sampling period. Furthermore, chloride to sulfate ratios (Figure 10b) were well above the value for seawater and the sulfate concentrations (Figure 9b) were below the threshold required to sustain SR. During November (Figure 19c) and December (Figures 20c and 20d), Mn^{2+} is no longer limited to the top 2 cm of sediment and is detected throughout the depth of the profiles at concentrations up to 100 μM. This appears to be another intermediate transition, as Mn reduction was not detected

during January (Figures 21c and 21d) and February (Figures 22c and 22d), indicating another shift in remineralization processes. Although methane concentrations were modest, the absence of other pathways leads to the assumption that this substation became methanogenic in surface sediments (Figure 8b).

Fe^{2+} was below detection in the marsh throughout the sampling year, which might suggest that Fe reduction is not a significant process in the marsh substation. Although this is a possibility, ample reactive solid phase Fe was measured in the marsh cores (Table 4). As seen in the intertidal region, the absence of dissolved Fe may be attributed to the formation of FeS (Howarth, 1984; Swider and Mackin, 1989; Taillifert et al., 2000). Aqueous FeS was detected from April through October, excluding June, and was almost always present throughout the entire depth of the profiles. Saturation states were calculated for the months where aqueous FeS, Fe^{2+}, and HS^- were all observed in a microelectrode scan (Sell, 2003). Although conditions were not favored for solid FeS to form, the presence of aqueous FeS not only has implications for Fe reduction, but for sulfide as well. These months were marked by excess dissolved sulfide, suggesting that SR occurs at higher levels than is conservatively accounted for here.

Marsh/Upland Edge

Prolific roots and rhizomes in the upper 20 cm of sediment in the marsh/upland edge cores impeded the depth to which profiles could be taken. Some of the root structures at this substation were woody and in a couple of cores actually broke off the electrode tips. These large root structures added another layer of complexity to this substation by intersecting the root and rhizome mat formed by other plant species. This inevitably influences the hydrology and porewater exchange processes.

Due to the large root presence and high water content of the marsh/upland edge, the sediments are easily influenced by climatic and hydrologic events. Biogeochemistry in the sediments from this substation reflected a drastic change due to a heavy rain event in November 2006 (Table 2). This was marked by a drastic drop in water content, reactive solid phase metals, and organic content.

Sediments at this substation exhibited the greatest small-scale heterogeneity within the cores, and the majority of the sampling months displayed the juxtaposition of suboxic and anoxic respiration products. September profiles (Figures 17e and 17f) demonstrated the classical biogeochemical depth profile, following the predicted thermodynamic sequence of reactions (Froelich et al., 1979). Mn^{2+} was detected (26 to 58 μM) in the surface 10 mm of sediments, followed by a section of overlap (between 4 and 10 mm) with Fe^{2+} building up and Mn^{2+} tapering off, and the profile ended with Fe^{2+} tapering off and a buildup of HS^- (74 μM).

Compared to the other two substations, the marsh/upland edge appears to have the most significant Fe reduction occurring over the depth of sediments sampled. The highest values for reactive solid phase Fe were measured from the marsh/upland edge cores (Table 5), consistent with the Fe oxyhydroxides which were often observed oozing from the sediments during core extraction. Fe^{2+} was detected in all profiles, except in March (Figure 11c) and April (Figures 12e and 12f). Most of the concentrations were measured below 75 μM; however, peaks of ~300 μM in July (Figure 15f) and ~750 μM were observed in October (Figure 18e). Aqueous FeS was detected in all but two months (June and November). As opposed to the other two substations, aqueous FeS was not detected through the entire depth of the upland profiles and was limited to depths between 1 cm and 4 cm. Dissolved Fe was typically observed in the surface 3 cm sediments, often overlapping the section where aqueous FeS was present. In the presence of

Fe^{2+}, HS^- was undetectable or at very low concentrations (<40 μM). Similarly, if HS^- was present, Fe^{2+} was below detection limits or at very low concentrations. Saturation states for FeS were calculated for the months where FeS, Fe^{2+}, and HS^- were all detected in microelectrode scans. As opposed to the other two substations, the substation U favored the precipitation of solid FeS during the month of October. Saturation states ranged from 2 to 11.

Sulfate concentrations (Figure 9c) remained close to the threshold concentration for sulfate reduction most of the year, and chloride to sulfate ratios (Figure 10c) varied considerably but generally indicated that SR had occurred. Salinity varied throughout the year, but was never over 1.82 (Table 5). Methane was present during many of the sampling months, indicating that the marsh/upland edge is the most methanogenic of all substations. Peaks in methane concentrations (Figure 8c) were observed during the fall and winter coinciding with increased chloride to sulfate ratios and low concentrations of sulfate, indicating that this substation became methanogenic during the winter.

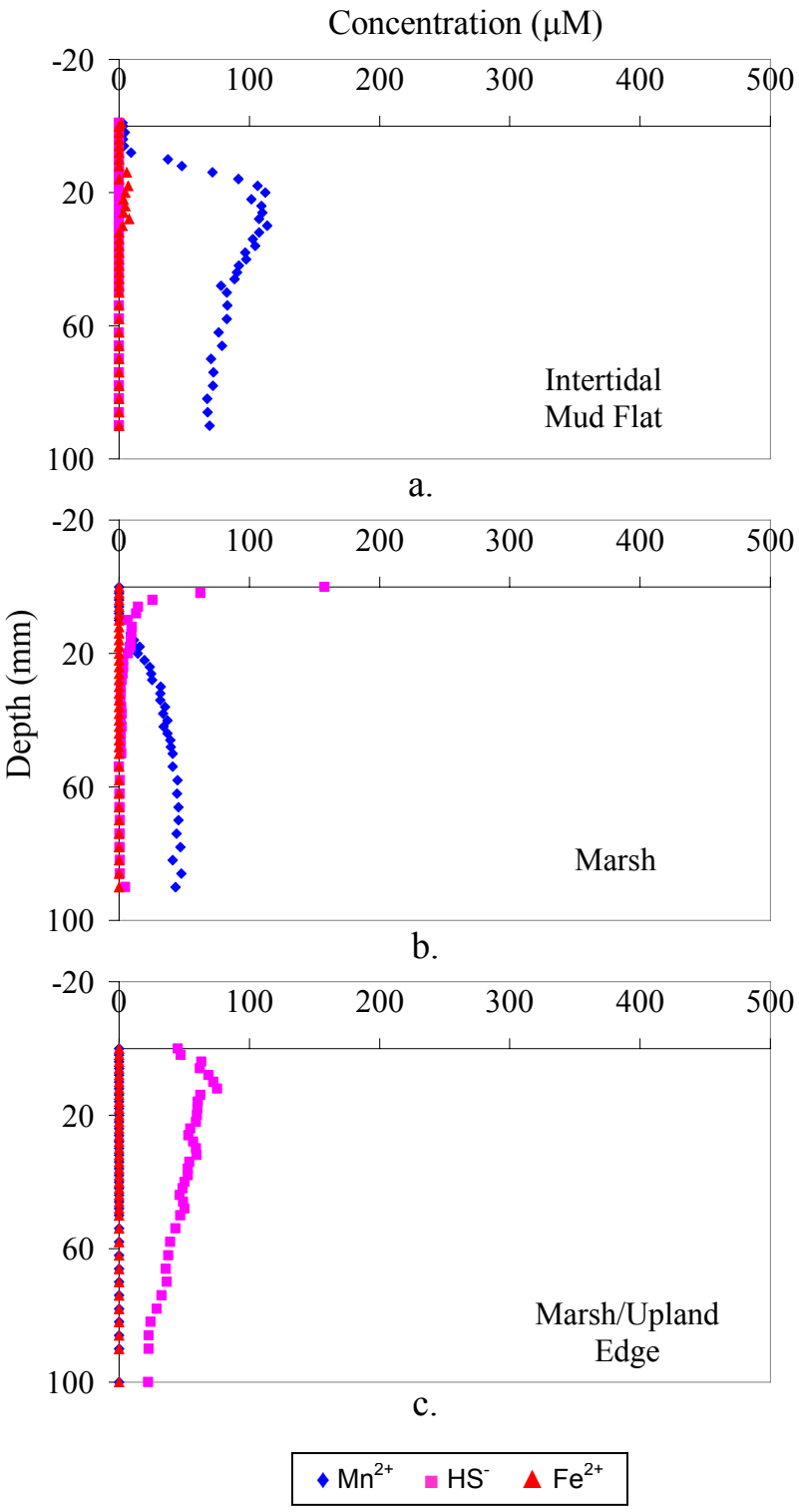

Figure 11. Depth profiles from April, 2006. Aqueous FeS was detected in the entire depth of profile c.

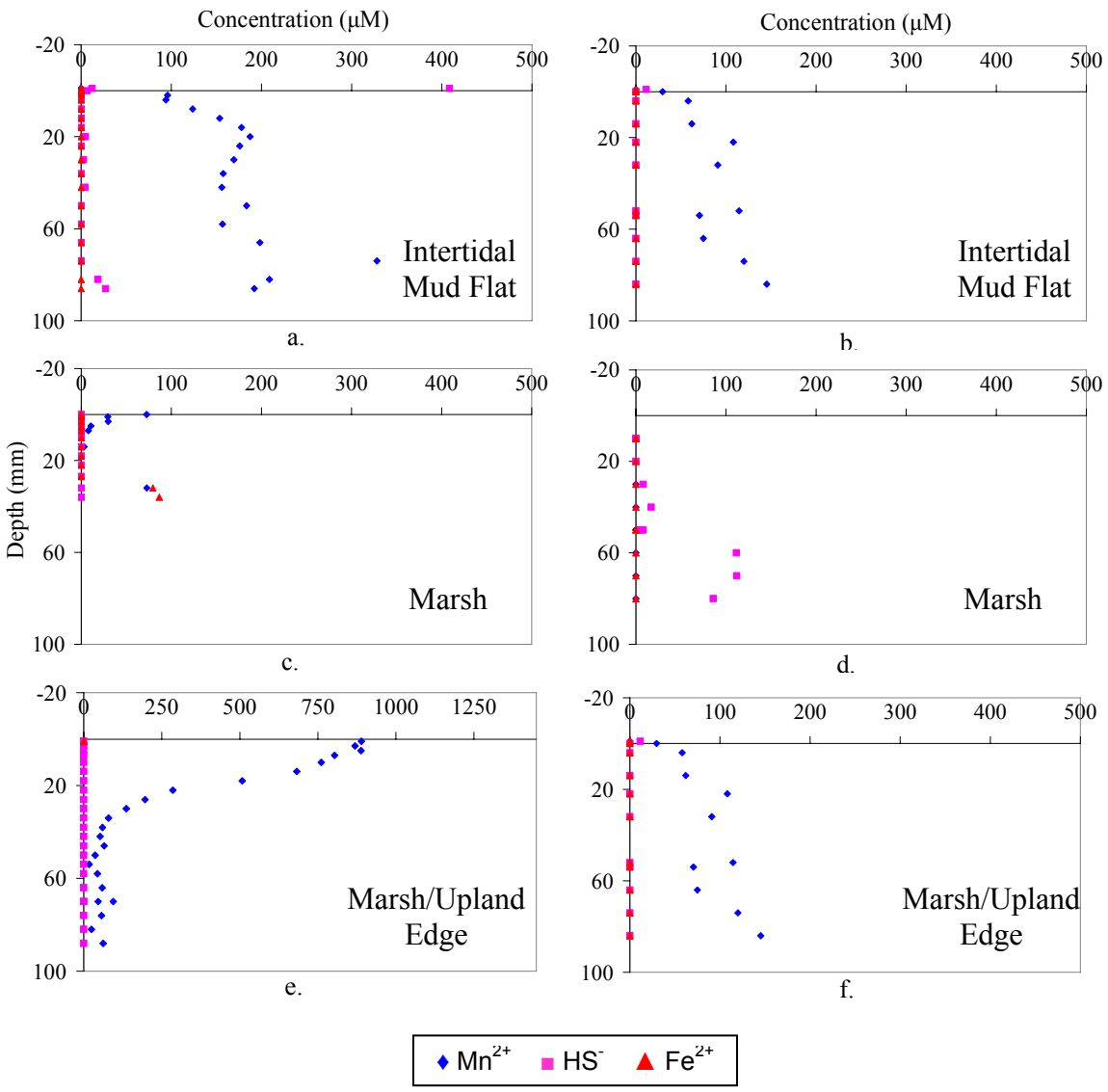

Figure 12. Depth profiles from April, 2006. The scale on graph e has been adjusted to account for higher concentrations. Aqueous FeS was detected from the surface to depth in all profiles.

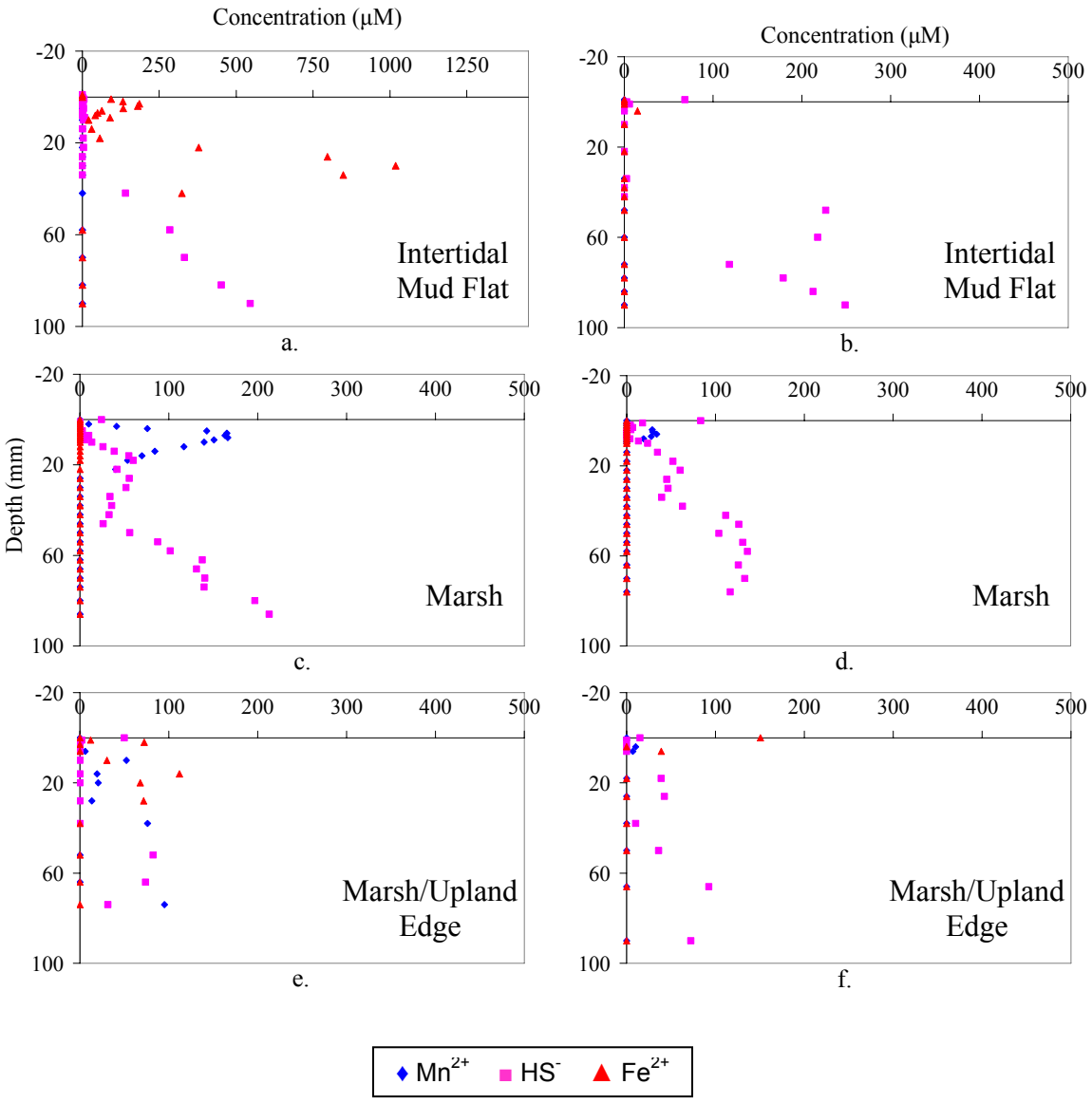

Figure 13. Depth profiles from May, 2006. The scale has been adjusted on graph a to account for higher concentrations. Aqueous FeS was detected in the surface to 8 mm in profile a and to 48 mm in profile b; at 38mm in profile e and continued to depth; in surface of c, d, and f and continued to depth.

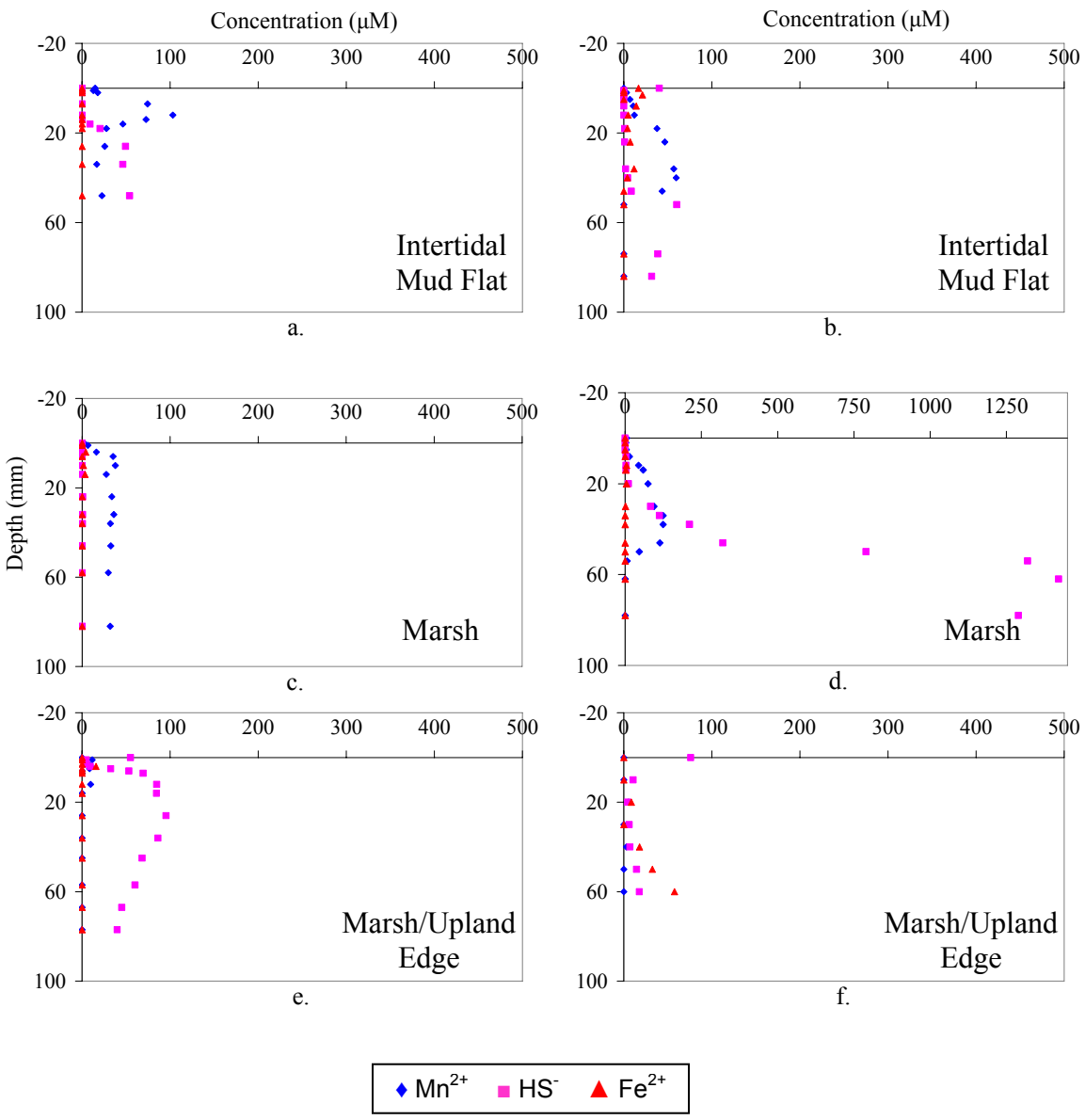

Figure 14. Depth profiles from June, 2006. The scale of the x-axis on graph d is different from the other graphs in order to account for higher concentrations of analytes. Aqueous FeS was not detected in any profiles.

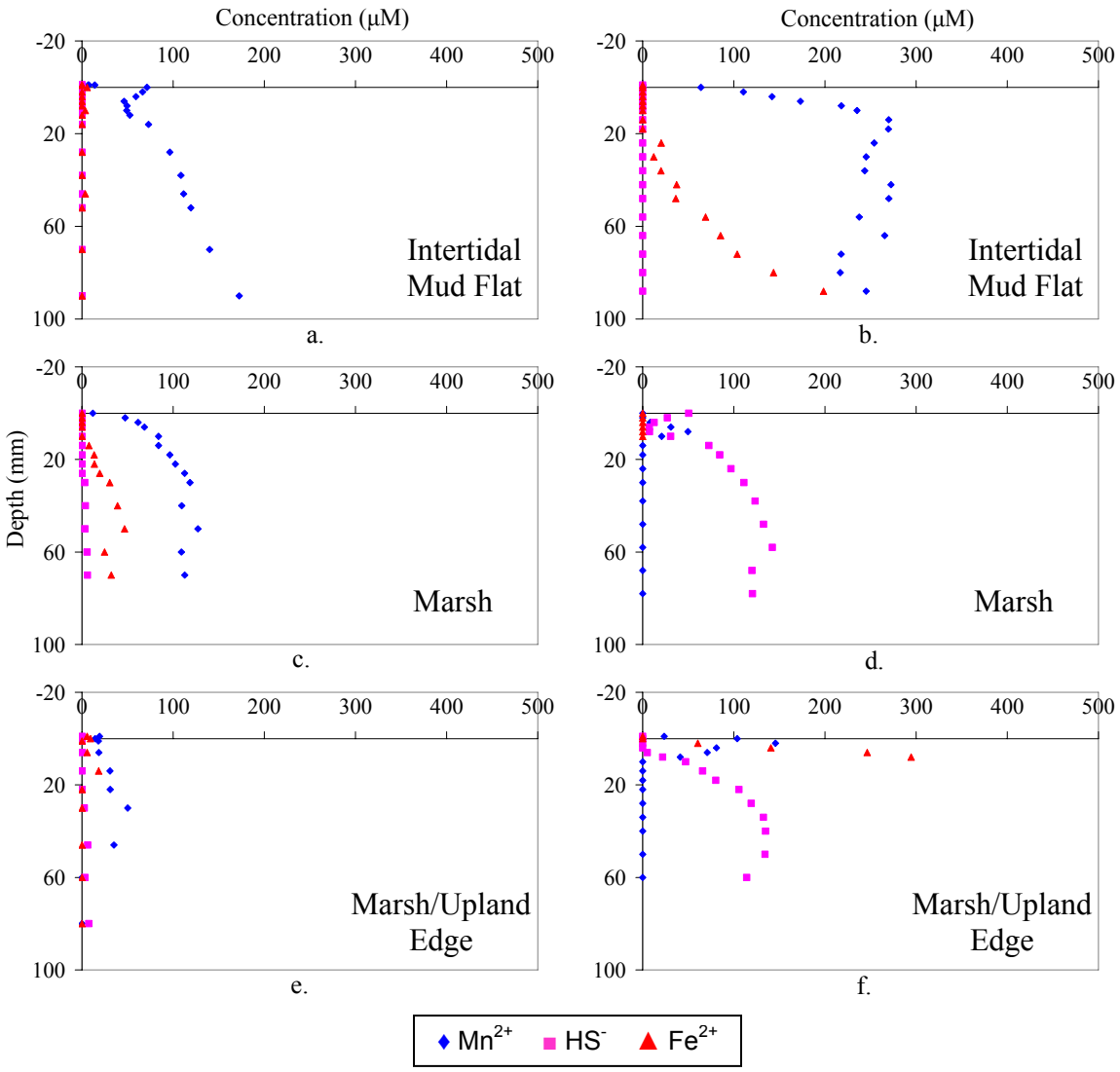

Figure 15. Depth profiles from July, 2006. Aqueous FeS was detected at 15 mm in profile d, 20 mm in profile e, and 10 mm in profile f; then continued to depth in all three profiles.

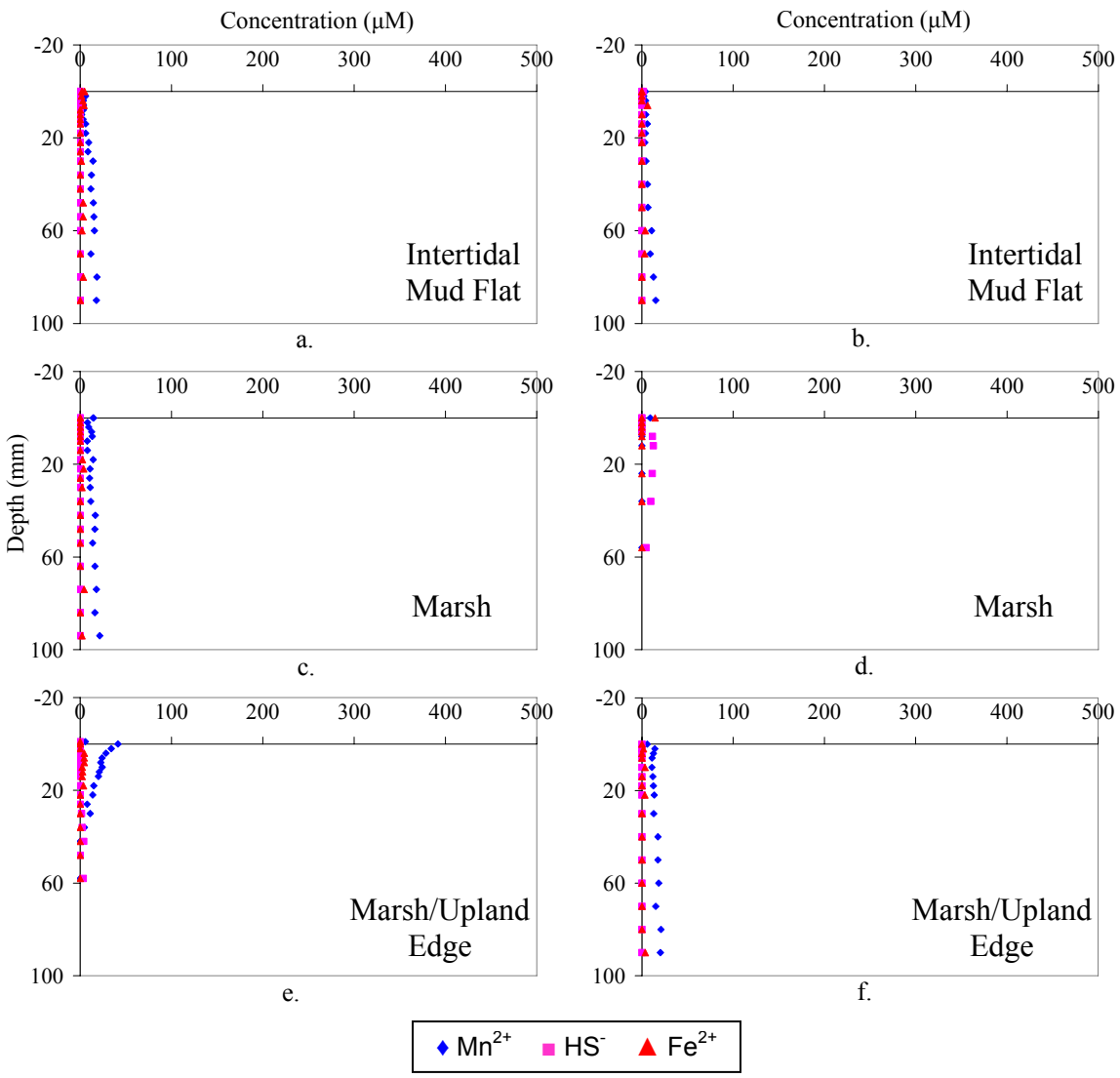

Figure 16. Depth profiles from August, 2006. Aqueous FeS was detected at 30 mm in profile c and 20 mm in profile e, then continued to depth in both; and in the entire depth of profile d.

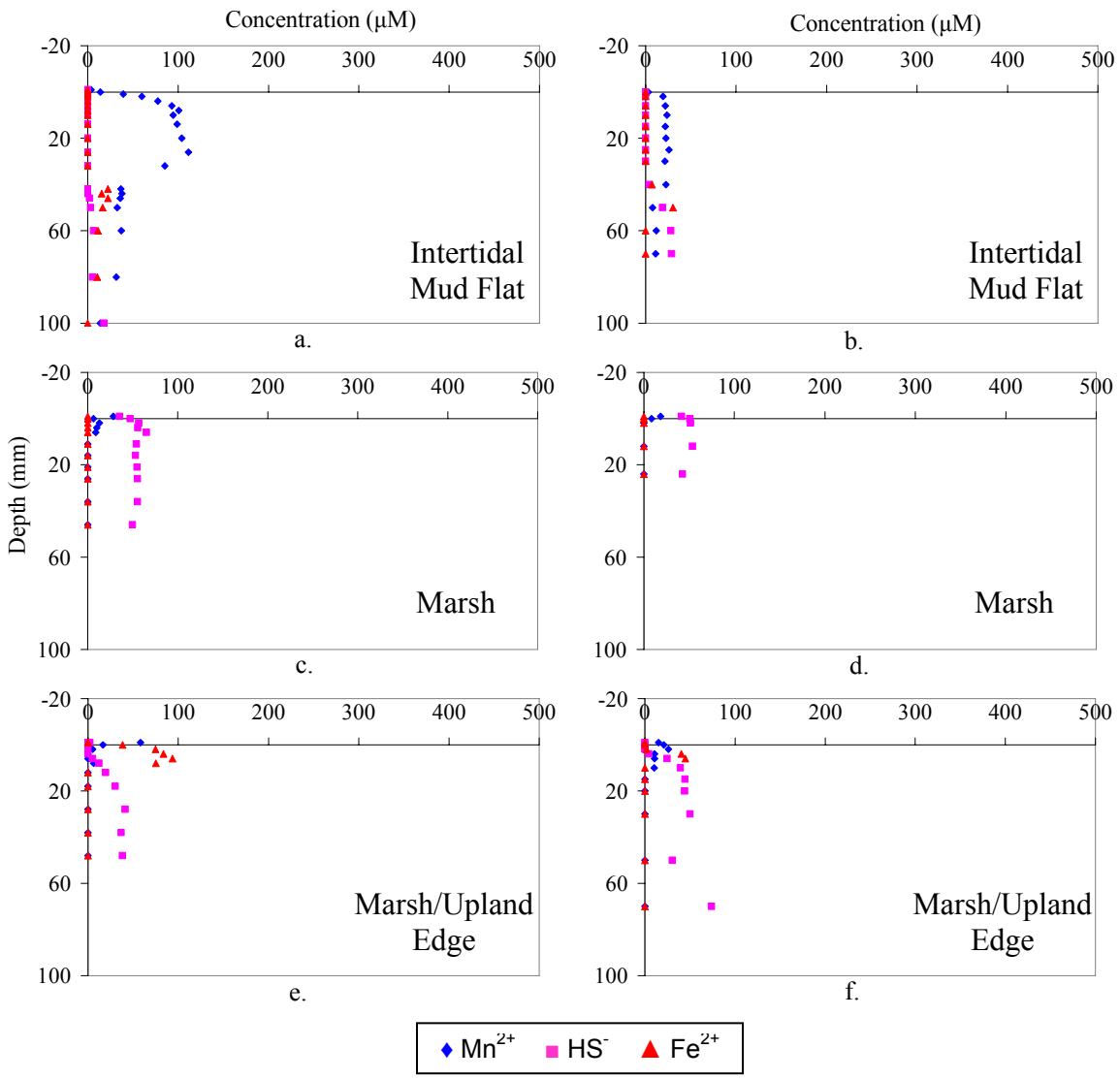

Figure 17. Depth profiles from September, 2006. Both profiles obtained from the marsh core ended as a result of hitting roots. Aqueous FeS was detected in the entire depth of profiles c and d; at 10 mm in profile f and then continued to depth.

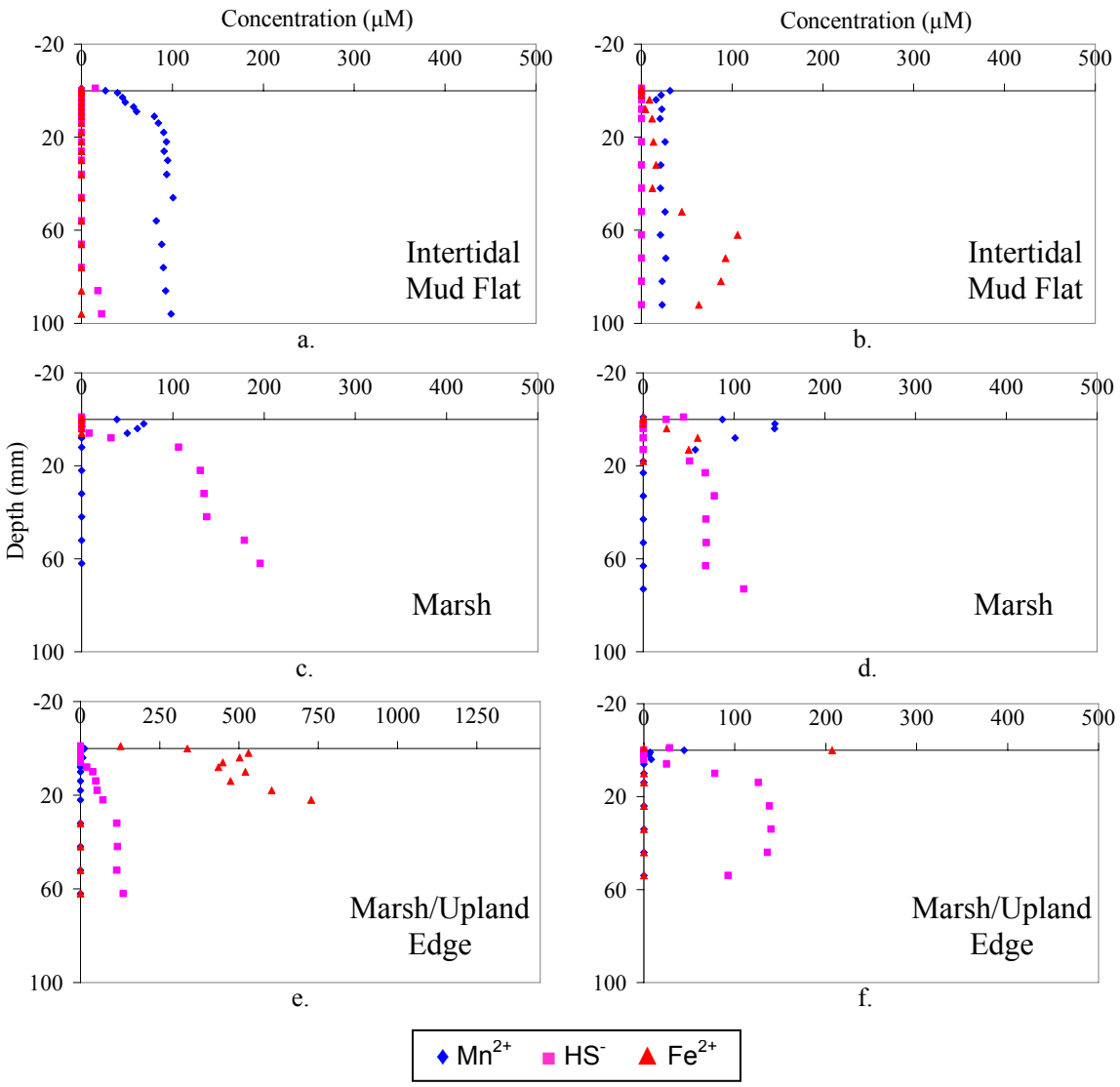

Figure 18. Depth profiles from October, 2006. The scale of the x-axis on graphs e and f is different from the other graphs in order to account for higher concentrations of analytes. Aqueous FeS was detected at 8 mm in profile c, 23 mm in profile d, 15 mm in profile e, 10 mm in profile f; then continued to depth in all.

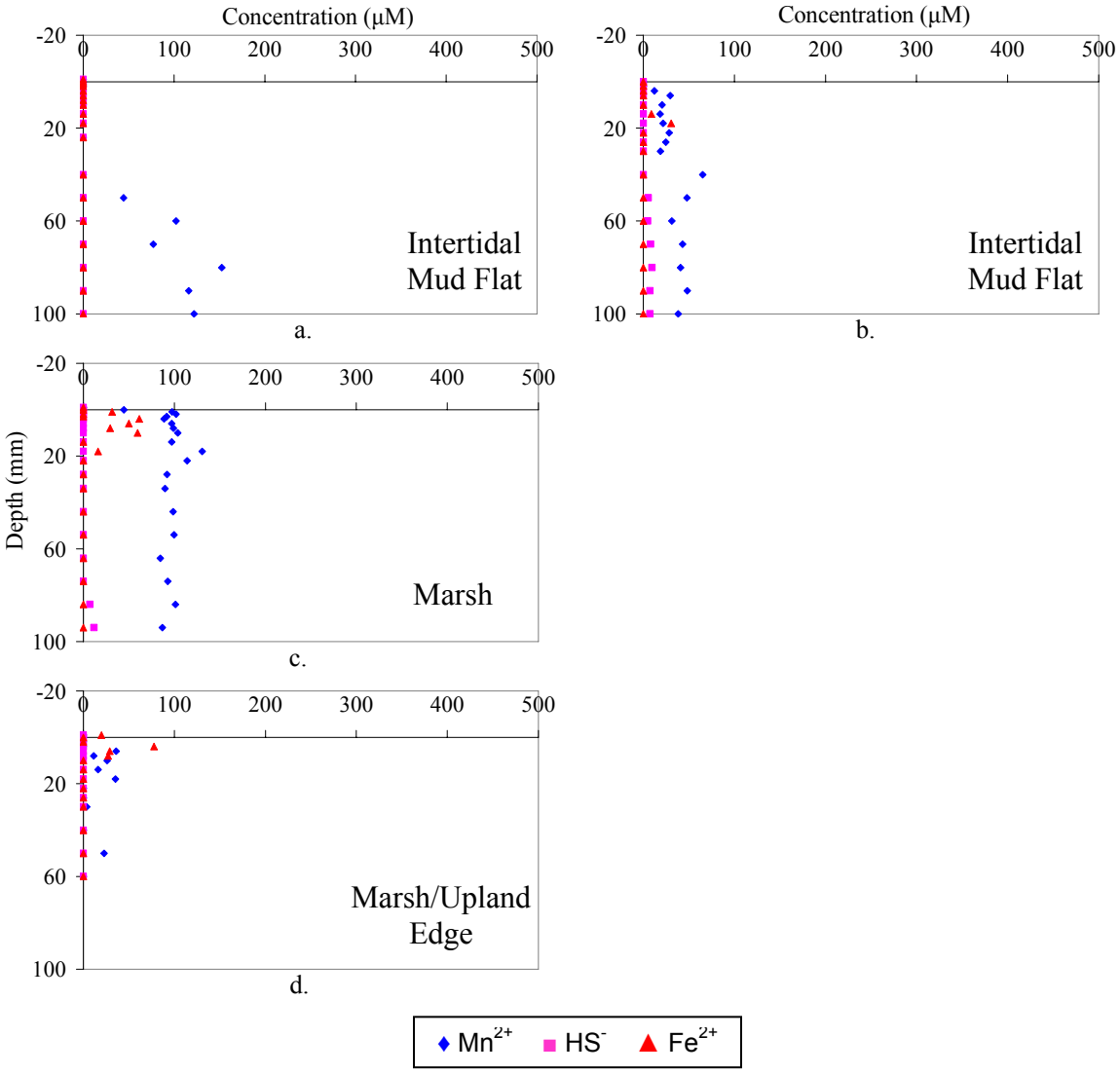

Figure 19. Depth profiles from November, 2006. Aqueous FeS was detected at the surface in the profile a and continued to a depth of 50 mm.

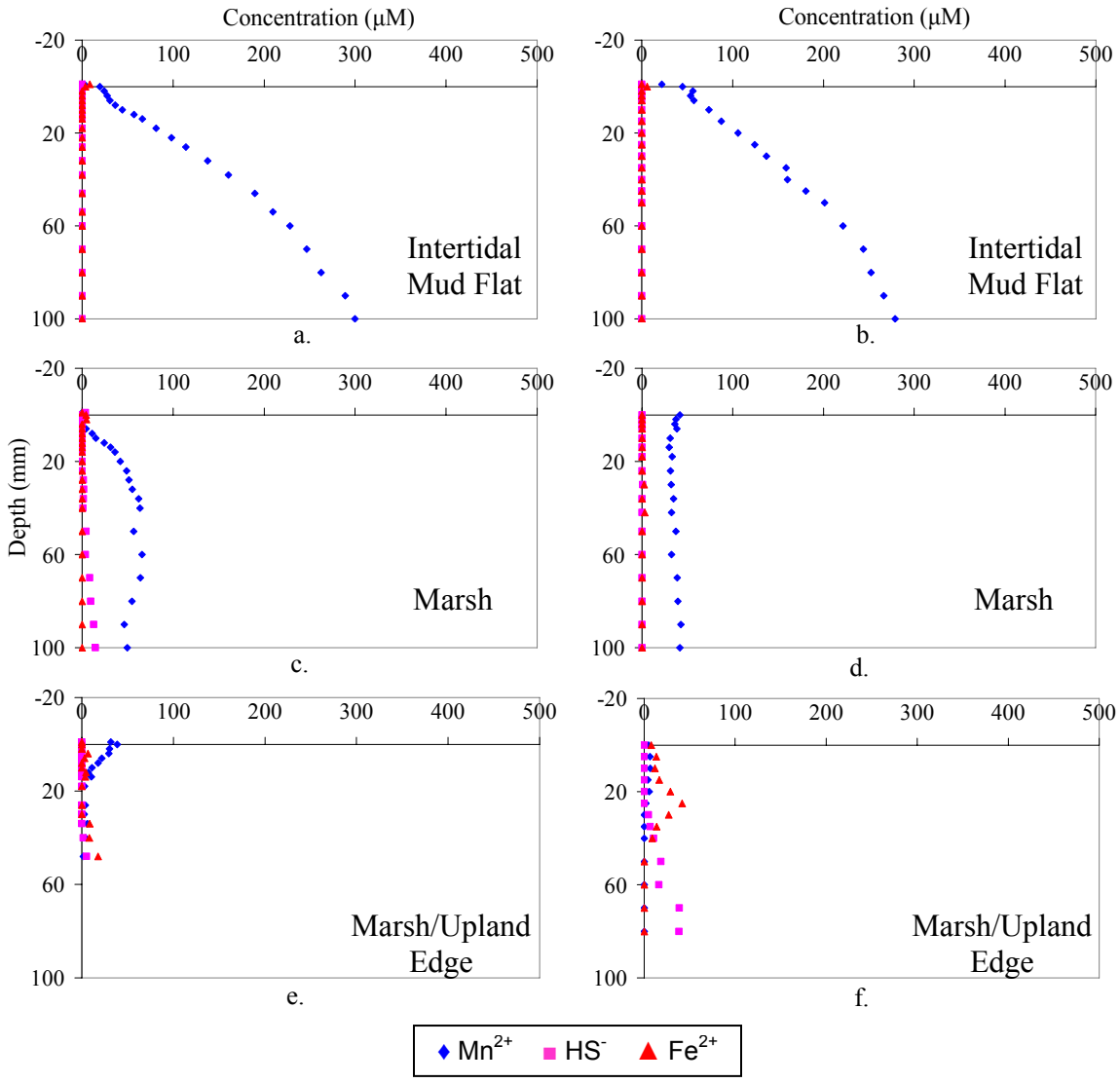

Figure 20. Depth profiles from December, 2006. Aqueous FeS was detected at 50 mm in profile f and continued to depth.

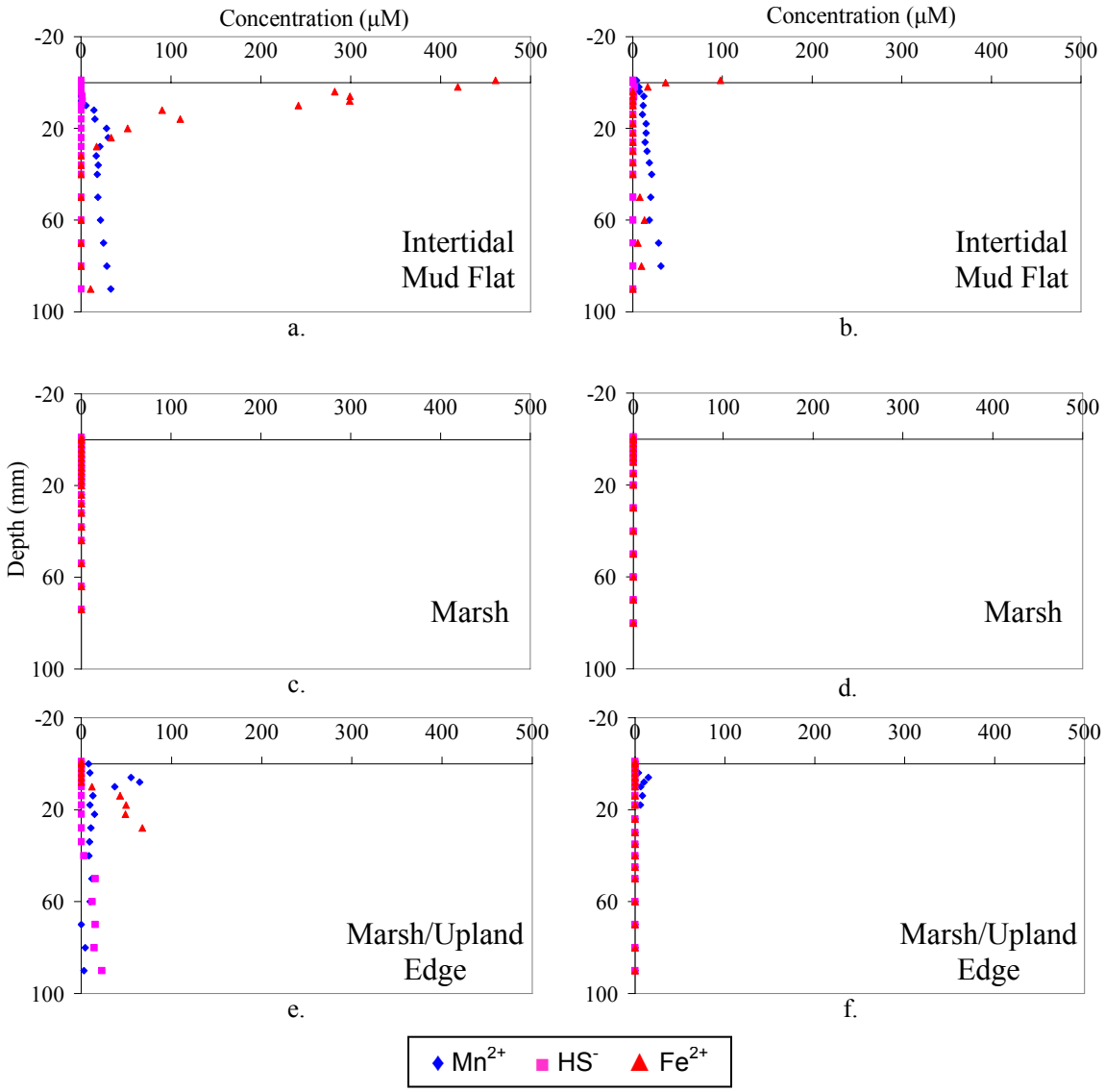

Figure 21. Depth profiles from January, 2007. Aqueous FeS was detected in the surface down to 10 mm in c, and the surface down to 4 mm in d; at 34 mm in e and continued to depth.

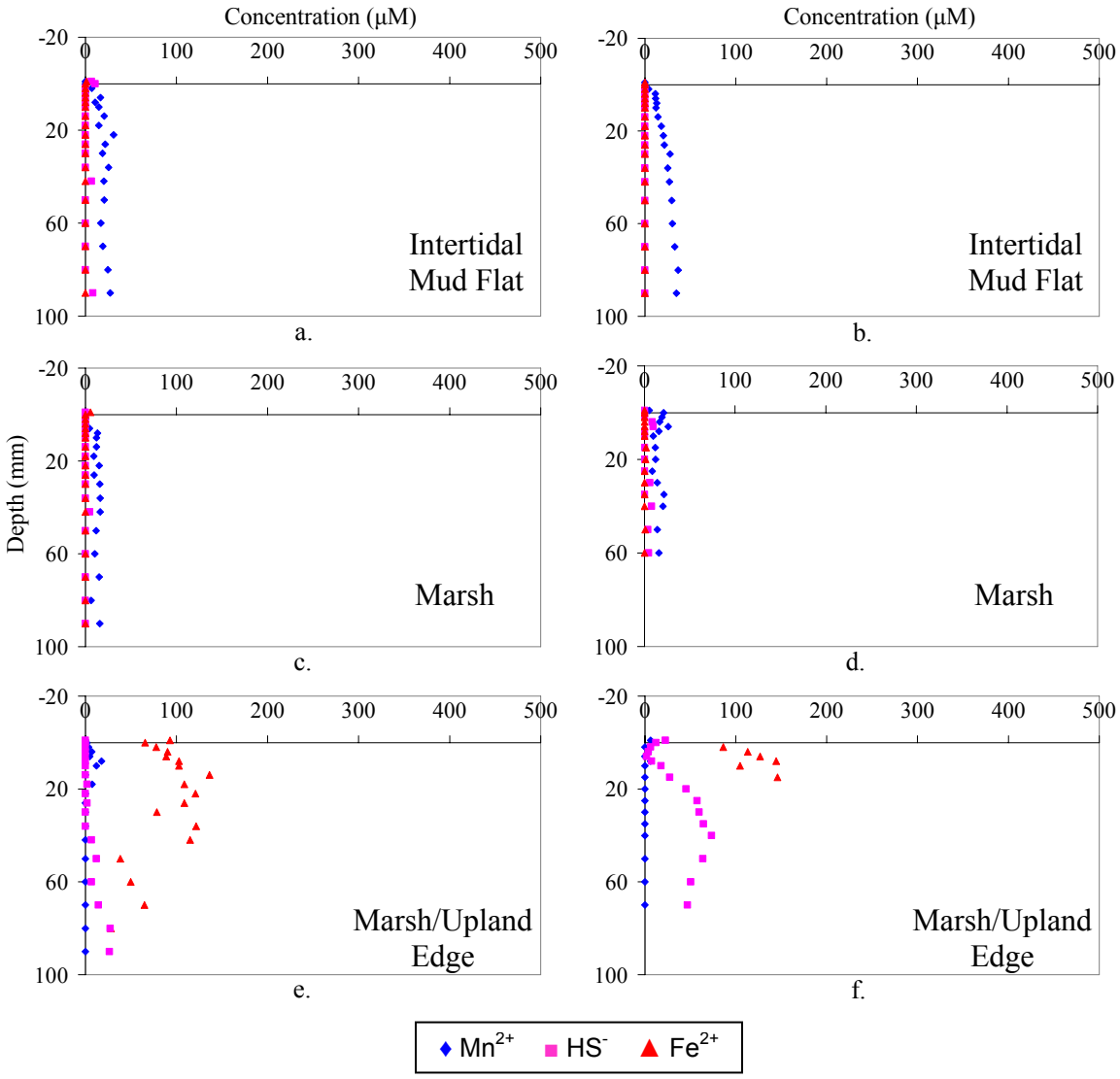

Figure 22. Depth profiles from February, 2007. Aqueous FeS was detected in the entire depth of profile b; at 90 mm in profile e and at 20 mm in profile f, then continued to depth.

CONCLUSIONS

Although it is impossible to determine whether Mn^{2+} is produced from bacterial or abiotic reduction, the results from this study have shown Mn reduction to be more important than expected based on the modest levels of reactive solid phase Mn that were present. Previous studies carried out in similar environments have often discounted the extent of Mn reduction, placing the emphasis on methanogenesis in freshwater marshes and sulfate reduction in salt marshes.

The products from Mn reduction appeared to dominate throughout the year in the intertidal mud flat substation, and this was often the only process detected throughout upper 10 cm of sediment that were investigated. The biogeochemistry reflected the relatively homogeneous texture of sediments at this substation, and the depth profiles within the same core showed remarkable similarities. Remineralization reactions were limited by a supply of organic matter which may have been completely utilized in the process of Mn reduction, leaving insufficient substrate for the next steps in the thermodynamic sequence.

Sediment biogeochemistry in vegetated sections of the marsh and marsh/upland edge was heavily influenced by sediment-root interactions, and therefore tended to show seasonality with respect to remineralization pathways. The marsh substation depth profiles revealed a vastly different biogeochemical sediment environment from the intertidal mud flat substation for this reason, and more so than the marsh/upland transition substation due to the larger woody roots present in this zone that are still active during the winter. Small-scale heterogeneity within cores was observed during the summer months but was absent during the winter months. Low reactive organic matter input during the winter resulted in similar biogeochemical patterns seen in the

intertidal mudflat substation, except with some evidence of Fe reduction. Depth profiles in the summer when reactive organic matter input was high displayed a more classical biogeochemical sequence of remineralization pathways (Mn^{2+} detection followed by Fe^{2+}, then HS^-).

The marsh/upland edge substation was highly influenced by subsurface hydrology, high organic content, and plant physiology which results in a biogeochemical mosaic of overlapping microenvironments dominated by different remineralization pathways (Mn reduction, Fe reduction, sulfate reduction, methanogenesis). The large root presence and high water content of this substation result a physically heterogeneous sedimentary environment, making the sediments more vulnerable to porewater flushing. The influence of tidal inundation, plant physiology, heavy rainfall events, and fluctuations in labile organic matter are reflected in the sediment biogeochemistry on a short time scale. Adding a layer of complexity to the hydrology, this portion of Eagle Island displays the characteristics of floating marshes (C. Hackney, personal conversation).

The overall, general trends observed across the landscape of Eagle Island (from the intertidal mud flat to the marsh/upland transition) include: increasing methanogenesis, increasing sediment heterogeneity, increasing content of organic matter, increasing water content, and increasing biogeochemical heterogeneity. Sites similar to Eagle Island, and its varied biogeochemistry, are likely to represent transitional environments expected to result from sea level rise. The great complexity of these environments, as described in this study, creates challenges for predicting the role that transitional wetlands will play in carbon storage and the release of greenhouse gases. This study demonstrated that Mn and Fe reduction may be more important than previously recognized. Whether this is a general phenomenon or site specific can not be determined without further research. Creating a baseline for comparison is crucial to

understanding how these systems function and therefore assess the ability for them to adapt to changing environmental conditions.

LITERATURE CITED

Aller, R. C. (1982) “The effects of macrobenthos on chemical properties of marine sediment and overlying water.” In McCall, P. L. & P. J. S. Tevesz (eds), Animal-sediment Relations. Plenum, New York: 53–102.

Aller, R. C. (1990) “Bioturbation and manganese cycling in hemipelagic sediments.” Philosophical Transactions of the Royal Society of London. Series A 331: 51–68.

Aller, R.C. (1994) “The sedimentary Mn cycle in Long Island Sound: Its role as intermediate oxidant and the influence of bioturbation, O_2, and C_{org} flux on diagenetic reaction balances.” Journal of Marine Research 52: 259-295.

Alongi, D.M., Sasekumar, A., Tirendi, F., and Dixon, P. (1998) “The influence of stand age on benthic decomposition and recycling of organic matter in managed mangrove forests of Malaysia.” Journal of Experimental Marine Biology and Ecology 225:197-218.

Berner, R. A. (1980) Early Diagenesis: a Theoretical Approach. Princeton University Press.

Brasse, S., Nellen, M., Seifert, R., and Michaelis, W. (2002) “The carbon dioxide system in the Elbe Estuary.” Biogeochemistry 59: 25-40.

Brendel, P.J. (1995) “Development of a mercury thin film voltammetric microelectrode for the determination of biogeochemically important redox species in porewaters of marine and freshwater sediments.” Ph.D. dissertation, University of Delaware, Newark, DE, 141p.

Brendel, P.J. and Luther, G.W., III (1995) “Development of a gold amalgam voltammetric microelectrode for the determination of dissolved Fe, Mn, O_2, and S(-II) in pore waters of marine and freshwater sediments.” Environmental Science and Technology 29: 751-761.

Brett, C.M.A and Brett, A.M.O (1998) Electroanalysis. Oxford University Press, Inc, New York.

Burdige, D.J. (1993) “The biogeochemistry of manganese and iron reduction in marine sediments.” Earth-Science Reviews 35: 249-284.

Canfield, D.E., Thamdrup, B., and Hansen, J.W. (1993) “The anaerobic degradation of organic matter in Danish coastal sediments. Geochimica et Cosmochimica Acta 57: 3867-3883.

Capone, D.G. and Bautista, M. (1985) “Direct evidence for a groundwater source for nitrate in nearshore marine sediments.” Nature 313: 214-216.

Capone, D.G. and Kiene, R.P. (1988) “Comparison of microbial dynamics in marine and freshwater sediments: contrasts in anaerobic carbon catabolism.” Limnology and Oceanography 33: 725-749.

Carr, A.P. and Blackley, M.W.L. (1986) "The effects and implications of tides and rainfall on the circulation of water within salt marsh sediments." Limnology and Oceanography 31:266-276.

Chanton, J.P., Whiting, G.J., Showers, W.J., Crill, P.M. (1992) "Methane flux from *Peltandra virginica*: stable isotope tracing and chamber effects." Global Biogeochemical Cycles 6:15-31.

Chapman, C. and Van Den Berg, C.G. (2005) "Microbenthic chamber with microelectrode for in-situ determination of fluxes of dissolved S(-II), I-, O2, Mn, and Fe." Environmental Science and Technology 39: 2769-2776.

de la Cruz, A.A. and Hackney, C.T. (1977) "Enegry value, elemental composition, and productivity of belowground biomass of a *Juncus* tidal marsh." Ecology. 58:1165-1170.

de Lange, G.J., Cranston, R.E., Hydes, D.H., and Boust, D. (1992) "Extraction of pore water from marine sediments: a review of possible artifacts with pertinent examples from the North Atlantic." Marine Geology 109: 53-76.

Devries, C.R., and Wang, F. (2003) "In situ two-dimensional high-resolution profiling of sulfide in sediment interstitial waters." Environmental Science and Technology 37:792-797.

Doumlele, D.G. (1981) "Primary production and seasonal aspects of emergent plants in a tidal freshwater marsh." Estuaries 4: 139-142.

Flemer, D.A., Heinle, D.R., Keefe, C.W., and Hamilton, D.H. (1978) "Standing crops of marsh vegetation of two tributaries of chesapeake bay." Esuaries 1: 157-163.

Froelich, P.N, Klinkhammer, G.P., Bender, M.L., Luedtke, N.A., Heath, G.R., Cullen, D., and Dauphin, P. (1979) "Early oxidation of organic matter in pelagic sediments of the eastern equatorial Atlantic: suboxic diagenesis." Geochimica et Cosmochimica Acta 43: 1075-1090.

Hackney, C.T., Posey, M., Leonard, L.L., Alphin, T., and Avery, G.B., Jr. (2006) "Monitoring effects of a potential increased tidal range in the Cape Fear River ecosystem dir to deepening Wilmington Harbor, North Carolina." Year 6: June 1, 2005-May 31, 2006. Report to Army Corps of Engineers, Wilmington District, Contract DACW 54-02-0009, 311p.

Hackney, C.T., Posey, M., Leonard, L.L., Alphin, T., and Avery, G.B., Jr. (2007) "Monitoring effects of a potential increased tidal range in the Cape Fear River ecosystem dir to deepening Wilmington Harbor, North Carolina." Year 7: June 1, 2006-May 31, 2007. Report to Army Corps of Engineers, Wilmington District, Contract DACW 54-02-0009.

Herbert, A.B., Morse, J.W., and Eldridge, P.M. (2007) "Small-scale heterogeneity in the geochemistry of seagrass vegetated and non-vegetated estuarine sediments: causes and consequences." Aquatic Geochemistry 13:19–39.

Hesslein, R.H. (1976) "An in situ sampler for close interval pore water studies." Limnology and Oceanography 21: 912-914.

Hines, M.E., Bazylinski D.A., Tugel, J.B. and Lyons W.B. (1991) "Anaerobic microbial biogeochemistry in sediments from two Basins in the Gulf of Maine: Evidence for iron and manganese reduction." Estuarine, Coastal and Shelf Science 32: 313-324.

Hines, M.E., Knollmeyer, S.L., and Tugel, J.B. (1989) "Sulfate reduction and other sedimentary biogeochemistry in a northern New England salt marsh." Limnology and Oceanography 34: 578-590.

Hoehler T. M. (1998) "Thermodynamics and the role of hydrogen in anoxic sediments," Ph.D. dissertation. University of North Carolina, USA.

Howarth, R.W. (1984) "The ecological significance of sulfur in the energy dynamics of salt marsh and coastal marine sediments." Biogeochemistry 1: 5-27.

Howarth, R.W., and Teal, J.M. (1979) "Sulfate reduction in a New England salt marsh." Limnology and Oceanography 24: 999-1013.

Howes, B.L., Howarth, R.W., Teal, J.M., and Valiela, I. (1981) "Oxidation-reduction potentials in a salt marsh: spatial patterns and interactions with primary production." Limnology and Oceanography 26: 350-360.

Howes, B.L., Dacey, J.W.H., and King, G.M. (1984) "Carbon flow through oxygen and sulfate reduction pathways in salt marsh sediments**."** Limnology and Oceanography 29: 1037-1051.

Howes, B.L., Dacey, J.W.H, and Wakeham, S.G. (1985) **"**Effects of sampling technique on measurements of porewater constituents in salt marsh sediments." Limnology and Oceanography 30: 221-227.

Howes, B.L., Dacey, J.W.H, and Goehringer, D.D. (1986) "Factors controlling the growth form of *Spartina alterniflora*: Feedbacks between above-ground production, sediment oxidation, nitrogen and salinity." The Journal of Ecology 74: 881-898.

Hussein, A.H., Rabenhorst, M.C., and Tucker, M.L. (2004) "Modeling of carbon sequestration in coastal marsh soils." Soil Science Society of America Journal 68: 1786-1795.

Jacobson, M.E. (1994) **"**Chemical and biological mobilization of Fe(III) in marsh sediments." Biogeochemistry 25: 41-60.

Jorgensen, B.B (1982) "Mineralisation of organic matter in the sea bed-the role of sulphate reduction." Nature 296: 643-645.

Jorgensen, B.B. and Sorensen, J. (1985) "Seasonal cycles of O_2, NO_3^-, and SO_4^{2-} reduction in estuarine sediments: the significance of an NO_3^- reduction maximum in spring." Marine Ecology Progress Series 24: 65-74.

Joye, S.B., Mazzotta, M.L., and Hollibaugh, J.T. (1996) “Community metabolism in microbial mats: the occurrence of biologically-mediated iron and manganese reduction.” Estuarine, Coastal and Shelf Science 43: 747–766.

Kelley, C.A., Martens, C.S., Chanton, J.P. (1990) “Variations in sedimentary carbon remineralization rates in the White Oak River Estuary, North Carolina.” Limnology and Oceanography 35:372-383.

King, G.M. (1988) “Patterns of sulfate reduction and the sulfur cycle in a South Carolina salt marsh.” Limnology and Oceanography 33: 376-390.

Koretsky, C.M., Meile, C., Curry, B., Haas, J., Hunter, K., and Van Cappellen, P. (2000) “The effect of colonization by *Spartina alterniflora* on pore water redox geochemistry at a salt marsh on Sapelo Island, GA.” Journal of Conference Abstracts 5: 599.

Koretsky, C.M., Meile, C., and Van Cappellen, P. (2002) “Quantifying bioirrigation using ecological parameters: a stochastic approach.” Geochemical Transactions 3: 17-30.

Koretsky, C.M., Moore, C.M., Lowe, K.L., Meile, C., Dichristina, T.J., and Van Cappellen, P. (2003) “Seasonal oscillation of microbial iron and sulfate reduction in saltmarsh sediments (Sapelo Island, GA, USA).” Biogeochemistry 64: 179-203.

Kostka, J. E. and Luter, G.W., III (1994) “Partitioning and speciation of solid phase iron in saltmarsh sediments.” Geochimica et Cosmochimica Acta 58: 1701–1710.

Kounaves, S.P. (1997) "Voltammetric Techniques" in Handbook of Instrumental Techniques for Analytical Chemistry. F.A.Settle (Ed.) Prentice Hall PTR, Upper Saddle River, NJ.

Kristensen, E. (2000) “Organic matter diagenesis at the oxic/anoxic interface in coastal marine sediments, with emphasis on the role of burrowing animals.” Hydrobiologia 426**:** 1–24.

Lovley, D. R. and Klug, M.J. (1986) “Model for the distribution of methane production and sulfate reduction in freshwater sediments.” Geochimica et Cosmochimica Acta 50: 11-18.

Lovely, D.R. and Phillips, E.J.P. (1986) “Organic matter mineralization with reduction of ferric iron in anaerobic sediments.” Applied and Environmental Microbiology 51: 683-689.

Lovely, D.R. and Phillips, E.J.P. (1988) “Manganese inhibition of microbial iron reduction in anaerobic sediments.” Geomicrobiology Journal 6:145-155.

Lovely, D.R. (1991) “Dissimilatory Fe(III) and Mn(IV) reduction.” Microbiological Reviews 55: 259–287.

Luther, G.W., III, Brendel, P.J., Lewis, B.L., Sundby, B., Lefrancois, L., Silverberg, N., and Nuzzio, D.B. (1998) "Simultaneous measurement of O_2, Mn, Fe, I^-, and S(II-) in marine pore waters with a solid-state voltammetric microelectrode." Limnology and Oceanography 43: 325-333.

Meites, L. (1965) Polarographic Techniques, 2nd edition. Wiley Interscience, New York.

Mendelssohn, I.A., McKee, K.L., and Patrick, W.H., Jr. (1981) "Oxygen deficiency in *Spartina alterniflora* roots: Metabolic adaptation to anoxia." Science 214:439-441.

Mendelssohn, I.A., and Postek, M.T. (1982) "Elemental analysis of deposits on the roots of *Spartina alterniflora*, Loisel." American Journal of Botany 69:904–912.

Mitsch, W.J. & Gosselink, J.G. (1993) "Wetlands." Van Nostrand Reinhold, New York, NY.

MRCSP (2005) Characterization of Geologic Sequestration Opportunities in the MRCSP Region Phase I Task Report, October 2003 – September 2005 pages 162-176.

Neubauer, S.C., Miller, W.D., and Anderson, I.C. (2000) "Carbon cycling in a tidal freshwater marsh ecosystem: a carbon gas flux study." Marine Ecology Progress Series 199: 13-30.

Odum, W.W. (1988) "Comparative ecology of tidal freshwater and salt marshes." Annual Review of Ecology and Systematics 19:147-176.

Rabenhorst, M. C. (1995) "Carbon storage in tidal marsh soils." pp 93-103. In R. Lal, J. Kimble, E. Levine, and B.A. Stewart (eds.) Soils and Global Change. Proceedings of the International Soil Symposium on Greenhouse Gases and Carbon Sequestration. Columbus, Ohio. April 5-9, 1993. Advances in Soil Science Series. Lewis Publishers, CRC, Boca Raton.

Reed, D.J. and Cahoon, D.R. (1999) "Response of coastal wetlands to future climate change and variability." pp 245-248. In D.B Adams (ed.) Proc. Specialty Conference on Potential Consequences of Climatic Variability and Change to Water Resources of the United States, May 10-12 1999, Atlanta, GA. American Water Resources Association.

Roden, E.E. and Wetzel, R.G. (1996) "Organic carbon oxidation and suppression of methane production by microbial Fe(III) oxide reduction in vegetated and unvegetated freshwater wetland sediments." Limnology and Oceanography 41: 1733-1748.

Schubauer, J.P. and Hopkinson, C.S. (1984) "Above- and belowground emergent macrophyte production and turnover in a coastal marsh ecosystem, Georgia." Limnology and Oceanography 20: 1052-1065.

Sell, K. (2003) "Temporal influences of seasonal hypoxia on sediment biogeochemistry in coastal sediments." Masters thesis, Texas A&M University, TX, 142p.

Sexton, S.G. (2002) “Rates of carbon remineralization in coastal wetland sediments under sulfate reducing and methanogenic conditions: implications for sea-level rise.” Master’s thesis, University of North Carolina, Wilmington, NC, 55p.

Sorensen, J., Jorgensen, B.B., and Revsbech, N.P. (1979). “A comparison of oxygen, nitrate and sulfate respiration in coastal marine sediments.” Microbial Ecology 5: 105-115.

Sundby, B. (2006) “Transient state diagenesis in continental margin muds.” Marine Chemistry 102: 2-12.

Sundby, B., Vale, C., Caçador, I., Catarino, F., Madureira, M.J., and Caetano, M. (1998) “Metal-rich concretions on the roots of salt-marsh plants: Mechanism and rate of formation.” Limnology and Oceanography 43:19–26.

Sundby, B., Vale, C., Caetano, M., and Luther, G.W., III (2003) “Redox chemistry in the root zone of a salt marsh sediment in the Tagus Estuary, Portugal.” Aquatic Geochemistry 9: 257-271.

Swider, K.T., and Mackin, J.A. (1989) “Transformations of sulfur compounds in marsh-flat sediments.” Geochimica Cosmochimica Acta 53**:**2311–2323.

Taillefert, M., Bono, A.B., and Luther, G.W., III (2000) “Reactivity of freshly formed Fe(III) in synthetic solutions and (pore)waters: Voltammetric evidence of an aging process.” Environmental Science and Technology 34: 2169-2177.

Teal, J.M., and Kanwisher, J. (1966) “Gas transport in the marsh grass, Spartina alterniflora.” Journal of Experimental Botany 17: 355-361.

Thamdrup, B., Fossing, H., and Jorgensen, B.B. (1994) “Manganese, iron, and sulfur cycling in a coastal marine sediment, Aarhus Bay, Denmark.” Geochimica et Cosmochimica Acta 58: 5115-5129.

Theberge, S.M. and Luther, G.W. (1997) “Determination of the electrochemical properties of a soluble aqueous FeS species present in sulfidic solutions.” Aquatic Geochemistry, 3: 191-211.

Valiela, I., Teal, J.M., and Persson, N.Y. (1976) “Production and dynamics of experimentally enriched salt marsh vegetation: belowground biomass.” Limnology and Oceanography 21:245-252.

Valiela, I., Teal, J. M., Volkman, S.B., Shafer, D., Carpenter, E. J. (1978) “Nutrient and particulate fluxes in a salt marsh ecosystem: tidal exchanges and inputs by precipitation and groundwater. Limnology and Oceanography 23:798-812.

Wang, T. and Peverly, J.H. (1999) “Iron oxidation states on root surfaces of a wetland plant (*Phragmites australis*).” Soil Science Society of America Journal 63:247-252.

Wang, Z.A. and Cai, W. (2004) “Carbon dioxide degassing and inorganic carbon export from a marsh-dominated estuary (the Duplin River): A marsh CO_2 pump.” Limnology and Oceanography 49:341-354.

Westrich, J.R. and Berner, R.A. (1984) “The role of sedimentary organic matter in bacterial sulfate reduction: The G model tested.” Limnology and Oceanography 29:236-249.

Whigham, D. F., McCormick, J., Good, R.E., and Simpson, R.L. (1978) “Biomass and primary production in freshwater tidal wetlands of the middle Atlantic coast.” pp 3-20. In R. E. Good, D. F. Whigham, and R. L. Simpson (eds.), Freshwater Wetlands: Ecological Processes and Management Potential. Academic Press, New York.

Yao, W. and Millero, F.J. (1996) Oxidation of hydrogen sulfide by hydrous Fe(III) oxides in seawater.” Marine Chemistry 52:1-16.

Yelverton, G. F., Hackney, C. T. (1986) “Flux of dissolved organic carbon and porewater through the substrate of a S*partina alterniflora* marsh in North Carolina. Estuarine Coastal Shelf Science 22:255-67.